Aus dem Institut Berlin Brandenburg Center für Regenerative Therapien
der Medizinischen Fakultät Charité – Universitätsmedizin Berlin

DISSERTATION

Development of a bioactive epicardial composite patch for support of myocardial regeneration

zur Erlangung des akademischen Grades
Doctor of Philosophy (PhD)

vorgelegt der Medizinischen Fakultät
Charité – Universitätsmedizin Berlin

von

Matthias Becker

aus Berlin

DATUM DER PROMOTION: .....[21.06.2020]

INHALT

ABSTRACT

After progression to heart failure, the only treatment option to date is a heart transplant, but this is limited due to a lack of donor organs. One response to a myocardial infarction is the activation of epicardial cells, ultimately differentiating towards the cardiac lineage in the myocardium.

One promising therapy, injection of progenitor cells in the infarcted area, has been met with contradictory success in the clinic. In contrast, epicardial patches, of polymeric or biological background, allow controlled local treatment to induce cardiac regeneration in preclinical attempts.

The aim of this project was to develop an epicardial composite patch to support the cardiac regeneration process. It consists of human cardiac extracellular matrix (hcECM), providing specific bioactivity and a polymeric or amniotic scaffold, with basic biocompatibility providing the required mechanical stability.

The hcECM was processed to a hydrogel (hgECM) and the scaffolds were coated with hgECM. Morphology and mechanical properties were measured determined. A hgECM coating caused a stabile nano-scaffold on the scaffolds and mechanical properties were unchanged. Then, transdifferentiated induced cardiomyocytes progenitors (iCMP) were cultured on the scaffolds to achieve a cellular bio enhancement.

After hgECM coating, biocompatibility was assessed by adhesion capacity, LDH-release, BrdU-incorporation and LIVE/DEAD staining. We found a clearly improved adhesion of several cardiac cells and iCMPs. Also, hgECM reduced cell necrosis and improved cell proliferation determined by LDH-release and BrdU-incorporation. Moreover, more alive cells were detected on hgECM coated scaffolds. ELISA technology revealed a reduction of pro-inflammatory cytokine secretion by LPS-activated monocytes on both hgECM coated scaffolds and by naïve monocytes on polymeric scaffold. No activation and impact by hgECM coating was observed regarding T cell proliferation and macrophage polarization determined by ELISA technology and flow cytometry.

Additionally, an in vitro assay was established based on the first response of the immune system: Polymorph Nuclear Cells. The amnion membrane as the “proof-of-principle” implant showed no immune response in this test and translation to any material is possible.

Here, we developed a new composite epicardial scaffold with hECM that has the potential to be used in large animal experiments and ultimately clinical studies. As a cell-free material, the production process can readily be scaled-up under GMP conditions. Further *in vivo* testing will reveal whether the composite patch is able to significantly modify post-infarct remodeling processes. In any event, it may serve as a universal platform for epicardial delivery of a broad spectrum of cells and therapeutic agents.

ABSTRAKT

Nach Fortschreiten der Herzinsuffizienz ist eine Herztransplantation bisher die einzige Behandlungsoption, die jedoch aufgrund fehlender Spenderorgane begrenzt ist. Eine Antwort auf einen Herzinfarkt ist die Aktivierung von Epikardzellen, die sich letztendlich zur Herzlinie im Myokard hin differenzieren können.

Injizierung von Vorläuferzellen in den Infarktbereich zeigten in der Klinik widersprüchlichen Erfolg. Im Gegensatz dazu ermöglichen Epikard-Patches mit polymerem oder biologischem Hintergrund eine kontrollierte lokale Behandlung, um die Regeneration des Herzens zu stärken. Dieses Projekt hatte die Entwicklung eines epikardialen Komposite-Patches zur Unterstützung des kardialen Regenerationsprozesses zum Ziel. Es besteht aus humaner extrazellulärer Herzmatrix (hECM), die eine spezifische Bioaktivität und eine optimale Zellumgebung bietet, und einem polymeren oder amniotischen Gerüst mit basaler Biokompatibilität, die die erforderliche mechanische Stabilität liefert.

Die hECM wurde zu einem Hydrogel (hgECM) verarbeitet, und Gerüste wurden mit hgECM beschichtet. Die grundlegende Morphologie und die mechanischen Eigenschaften wurden durch einachsige Ziehversuche und Elektronenmikroskopie gemessen. Die Biokompatibilität wurde durch Adhäsionskapazität, LDH-Freisetzung, BrdU-Einbau und LIVE/DEAD-Färbung bewertet und die Immunogenität wurde durch Zytokinsekretion, Makrophagenpolarisation und T-Zellproliferation bestimmt. Darüber hinaus wurden transdifferenzierte induzierte Kardiomyozyten-Vorläufer (iCMP) auf Gerüsten zur zellulären Bioverbesserung kolonialisiert. Eine hgECM-Beschichtung bewirkte eine stabile Nanobeschichtung auf den Gerüsten und die mechanischen Eigenschaften wurden nicht beeinflusst. Nach der hgECM-Beschichtung verbesserte sich die Adhäsion bei mehreren Herzzellen und iCMP deutlich. Darüber hinaus induzierte hgECM eine verringerte Zellnekrose und verbesserte Zellproliferation, bestimmt durch LDH-Freisetzung und BrdU-Einbau. Durch LIVE/DEAD-Färbung wurden auf hgECM-beschichteten Gerüsten mehr Zellen als lebendig indentifiziert. Eine hgECM-Beschichtung verursachte eine Verringerung der proinflammatorischen Zytokinsekretion bei LPS-aktivierten Monozyten auf beiden Gerüsten und auch von naiven Monozyten auf polymeren Gerüsten. In Bezug auf die Proliferation von T-Zellen und die Polarisation von Makrophagen wurde keine Aktivierung und keine Beeinflussung durch hgECM-Beschichtung beobachtet.

Zusätzlich wurde ein *in vitro* Test basierend auf der ersten Reaktion des Immunsystems etabliert: Polymorph Nuclear Cells. Die Amnionmembran als „Proof-of-Principle“ -Implantat zeigte in diesem Test keine Immunreaktion, und eine Translation auf jedes Material ist möglich. Wir haben hier ein neues zusammengesetztes Epikard-Gerüst mit humaner Herz-ECM entwickelt, das das Potenzial hat, in Großtierstudien und schließlich in klinischen Studien eingesetzt zu werden. Als zellfreies Material kann der Produktionsprozess unter GMP-Bedingungen problemlos skaliert werden. Weitere *in vivo* Tests zeigen, ob das Komposit-Pflaster Post-Infarkt-Remodellierungsprozesse signifikant modifizieren kann. In jedem Fall kann es als universelle Plattform für die epikardiale Abgabe eines breiten Spektrums von Zellen und Therapeutika dienen.

INTRODUCTION

Myocardial infarction

In the western world, cardiovascular disease (CVD) is one of the leading causes of death[1]. Women are more frequently affected than men, and myocardial infarction (MI) - a subgroup of CVD - is more common on its own than lung cancer or respiratory diseases[2]. There is no cure at present, since no therapy is available that can restore the function of the heart. For a short time, a left ventricular assist device (LVAD) can be used to support the cardiac function externally. However, the only effective current "therapy" for end-stage heart failure patients is a heart transplant. Even though it is a complex surgery, has the risk of rejection and requires immunosuppressive medication, so far it is the gold-standard to restore cardiac function. Yet the availability of donor organs is severely limited[3]. Therapeutic options are palliative only because the postnatal heart has almost lost its ability to regenerate and cardiomyocytes (CM) can only minimally proliferate[4–7]. Therefore, research is trying to develop strategies to support the endogenous regenerative ability to heal the damaged myocardium.

An MI is the result of a rupture of an atherosclerotic plaque and the subsequent occlusion of a coronary artery[8]. The lack of oxygen and nutrients results in damage to the cardiac tissue. Operative or drug interventions can reopen the vessel and prevent life-threatening damage to the heart. Dying cells - a common concomitant of MI - result in the release of various chemo- and cytokines, whereupon various immune cells, such as neutrophils and monocytes, are attracted, triggering the first phase of healing - inflammation. It leads to the formation of a granulation tissue[9]. The infiltrated immune cells remove dead cells and release matrix metalloproteinases (MMP), which degrade the extracellular matrix (ECM) in order to facilitate cell infiltration and migration. In addition, fibroblasts begin to form ECM and thereby strengthen the tissue[9,10]. The pro-inflammatory reaction is resolved by release of anti-inflammatory cytokines and the switch of pro-inflammatory/M1 macrophages to anti-inflammatory/M2 macrophages [11]. These macrophages aid in the proliferative phase, where the release of angiogenic factors induces blood vessel formation at the infarction border zone. Because cardiomyocytes died during MI and ECM is reduced by MMPs, the cardiac wall is weakened. This is compensated by proliferating (myo)fibroblasts that strengthen the wall by ECM production, but since hardly any new cardiomyocytes are formed, this results in the formation of a collagen rich, non-functional scar.

Current strategies for cardiac regeneration

Initially, there was a concentrated focus on injecting various stem or progenitor cells into the infarcted tissue. *In vitro* results showed cardioprotective effects *in vitro*[12], and pre-clinical *in vivo* studies corroborated these results with an effect on cardiac function. Since then, there have been few applications in clinical trials, but results have been ambiguous[13].

An obvious explanation for the lack of effect in the clinic is that cell retention is extremely low and the majority of the injected cells only survive a short time[14,15]. Thus, although pure cell injection has shown some effect, there is a great need for improvement in order to be effective in the clinic. One approach is to sort the cells into layers and then stretch them over the epicardium. If, for example, stem cell derived cardiovascular cells are arranged in multiple layers and these sheets are used as epicardial coating, then an increase in engraftment and survival is observed[16]. Another strategy is cell embedding into biomaterials such as collagen or fibrin. Studies have shown that gels containing cells and applied intramyocardially as well as epicardially resulted in improvements in cardiac remodeling and preservation of cardiac function [17–19]. This means that the existing regenerative strategies do not need to be discarded, but specific improvements are needed for successful translation, such as optimized embedding or epicardial applications.

The role of the Epicardium in regeneration

A consequence of the ischemic injury to the heart during MI, is activation of the epicardium. It shows increased proliferation and forms a thickened layer that can spread over the infarcted zone[20]. By expressing diverse genes that play an important role in cardiac development, this layer contributes to cardiac regeneration. Epicardial progenitors undergo a so-called Epithelial-to-Mesenchymal Transition (EMT), after which they migrate into the myocardium and there differentiate towards the cardiac lineage[21]. One of the major players identified during this process is thymosin beta-4 (Tβ4) [22]. It activates the protein kinase C (PKC) and integrin-linked kinase (ILK) and was identified to induce neovascularization, cardiac repair and activation of the epicardium even in adult mammals[23–25]. This effect in combination with CM proliferation explains the observation that neonatal mammals are able to regenerate a MI completely without scar[6], and the importance of the epicardium in postnatal mammals as Tβ4 application can extend that regenerative window up to 7 days, specifically by activating epicardial cells [26]. In addition, isolated epicardial cells (epicardial derived cells; EPDCs) can spontaneously perform EMT *ex vivo* [27]. These cells then secrete a variety of paracrine factors that exhibit cardio protective properties [28].

This observation clearly shows that the epicardium and epicardial cells play a prominent role during regeneration. Even though the regenerative potential of the epicardium is reduced in adults, it can still greatly support cardiac regeneration [21], which is why the epicardium is a very attractive target for the development of new therapeutic strategies.

Patch design

Patches are well suited to induce cardiac regeneration by supporting the activated epicardium. They can be designed to completely coat the infarcted area. Patch production has benefited from electrospinning technology, as it can produce a large variety of patches with diverse properties, as standardized as possible. For example, fiber diameter or orientation can be changed almost arbitrarily and therefore cardiac patches with very different properties can be produced. The stiffness parameter is one of the most important characteristics of a patch because an epicardial scaffold has to withstand suturing and the forces of the heart during contraction after it has been attached to the epicardium. Integration of a bioactive component such as gelatin during the spinning process can improve cell response or cardiomyocytes proliferation[29]. However, it can have a dramatic impact on the final stability of the patch and possibly even affect its clinical application. Nevertheless, although stiffness, tensile strength and elastic modulus may be strongly influenced, previously designed patches have met the minimum criteria to be applied epicardially[30].

Much more important is the architecture of the patches[31]. In the past, various patches have been designed that have shown an effect on angiogenesis, proliferation and attachment of cardiomyocytes, human umbilical vein endothelial cells (HUVECs) or smooth muscle cells (SMCs) *in vitro* [32–35]. In addition, beating cardiomyocytes can be maintained on a patch [36]. Despite that polymers, e.g. polycaprolactone (PCL), allow a multitude of patch preparations, any polymer may eventually induce inflammation *in vivo*, for example by skewing the ratio of M1 to M2 macrophages[37].

On the one hand, the use of epicardial scaffolds based on a polymer has the advantage that they can be produced in a very standardized and defined manner. On the other hand, they have the disadvantage of the aforementioned inflammatory risk, but another disadvantage is that the material is specifically designed to address a small range of therapeutic targets. That is, each of these materials has unique advantages and disadvantages in terms of regeneration. For this reason, the use of biological patch materials, such as human amniotic membrane (AM) is a biologically more attractive alternative. For this material, a variety of regenerative aspects is already known. For decades it has been used in different aspects of regeneration [38–40]. In addition, a clear improvement of cardiac function upon infarction was also observed after epicardial application of the cell-free AM (DeAM), in comparison to cell-containing AM before and after inducing EMT[41], which is known to be beneficial in case of intramyocardial application of amnion epithelial cells[42].

This results not only highlight the effect of an epicardial patch after myocardial infarction, but also show the importance of optimal patch design.

The importance of the Extracellular Matrix

Like any organ, the cells of the heart are embedded in a unique structure that allows cell adhesion while providing strength and flexibility: the ECM. It consists of connective parts such as collagen (interstitial matrix) as well as cell surrounding components (pericellular matrix). Furthermore, the human cardiac ECM (hcECM) has an influence on differentiation, proliferation and apoptosis of cells[43,44]. The ECM also significantly influences diverse signaling pathways. For example, the cell-ECM interactions by integrins and the so-called focal adhesion kinase[45] play an important role in cardiac development[46]. Intracellular integrin kinase has diverse pro-survival effects in cardiac cells[23] through the AKT pathway[47]. This means that the ECM not only provides stability, but also presents various stimuli to create an optimal cell environment. Therefore, the ECM has become a focus point of regenerative therapies due to its multitude of regenerative aspects. For example, it was shown early on that a hydrogel from the porcine urinary bladder ECM increases the viability of SMCs[48]. Several studies describe the production of ECM hydrogels from various organs[49] and application as coating solution[50]. Moreover, direct injection of cardiac ECM hydrogel into the myocardium in large animal model showed regenerative effects[51,52].

Composite materials may help differentiate stem or progenitor cells, but so far such approaches have only been performed with animal ECM [53,54]. With focus to the future clinical translation, there is the risk of implantation of a xenograft instead of allograft – the immune reaction of each implanted object is already an important point[55] – plus, human cardiac ECM differs between human and swine, which can make a difference in the final clinical success[56].

So far, the observed effects and applications of the ECM are only intramyocardial and the power of the epicardium is completely bypassed in the regeneration process. In other words, there is a need to design a composite material that consists of a biomaterial for the requisite stability of the epicardial suturing and basal cytoprotective properties while containing species and organ specific ECM for optimal cell interaction. If the gap between the positive biological properties of the ECM and biopolymers with defined stability can be closed, the regenerative potential of an epicardial patch can be redefined and applied.

Aim

The aim was to design an epicardial ECM composite patch for cardiac regeneration. A polymer specifically designed for cardiac applications was used, consisting of caprolactone and dioxanone (PEEU). In comparison, DeAM represents a biological scaffold. The study was divided into four objectives:

1. Combination of the scaffolds with human cardiac ECM hydrogel (hgECM) to improve the embedding of cells or bioactive molecules.
2. Determination of basal mechanical properties, *in vitro* biocompatibility, and assessment of immunogenicity.
3. Implementation of induced cardiomyocate progenitors (iCMP) designed by transdifferentiation for cellular enhancement.
4. To address immunological behavior of implants, a rapid assay based on the behavior of polymorph nuclear cells (PMNs) was established and tested with amniotic patch constructs.

These constructs were established and tested *in vitro* to optimize the patches and ultimately pave the way for *in vivo* applications to improve left ventricular cardiac function in a murine model of MI.

MATERIAL AND METHODS

Decellularization and ECM processing

Human full term placentas were anonymously obtained after cesarean delivery of healthy and uncomplicated pregnancies from women who had given written informed consent for use of the placenta for research purposes. Excessive blood was washed off and the AM was mechanically peeled from the underlying chorion, washed to remove blood and decellularization was performed by incubation in Tris/EDTA and SDS-solutions, followed by another wash resulting in DeAM. Detailed information can be found in[57].

Left ventricular myocardium was collected from explanted hearts from patients who underwent heart transplantation for end-stage dilated cardiomyopathy. Patients provided informed consent for the use of the tissue for research purposes, and the process of tissue collection was approved by the Institutional Review Board and ethics committee of Charité-Universitätsmedizin Berlin. Cardiac tissue was cut into cubes of approximately 1x1x1 cm and subsequently sectioned into 300 µm thick slices, followed by incubation in Tris/EDTA and SDS-solutions. Remaining DNA was removed by incubation in serum. Resulting ECM was lyophilized, milled towards a powder and digested to a homogeneous solution by a pepsin-based protocol, resulting in hgECM. Detailed information can be found in[58].

Mass spectrometry

The hgc was dissolved in Tris-buffer and sonicated on ice. Urea buffer was added and incubated at room temperature. The solution was transferred onto an amicon-filter followed by buffer exchange to trypsin and incubated at 37 °C overnight. Subsequently, amnion bicarbonate-buffer was added and the solution centrifuged at room temperature. The flow-through was desalted and peptide samples were dried and extracted in trifluoroacetic acid. Analysis was performed using UPLC ESI-QTOF-mass spectrometer. Mass spectra were evaluated using MASCOT software, automatically searching the SwissProt 51.9 database. No fixed modifications were considered. Only proteins with scores corresponding to $p < 0.05$ were considered. The cut-off score for individual peptides was equivalent to $p < 0.05$ for each peptide as calculated by MASCOT. Detailed information can be found in[57].

Patch preparation

DeAM and PEEU (kindly provided by Andreas Lendlein, AG Ma and AG Kratz from Institute of Biomaterial Science, Helmholtz-Zentrum Geesthacht, Teltow, Germany) were cut into circles with a diameter of 8 mm using a biopsy punch. Patches were placed into 48 well plates and covered with hgECM (150µl/cm²). Covered patches were completely dried and washed, resulting in hgECM covered DeAM and PEEU (DeAM+E and PEEU+E, respectively). Detailed information can be found in[57].

Scanning electron microscopy

Samples were fixed with 2.5% grade I glutaraldehyde and dried using incubation steps in increasing ethanol concentration (30%, 50%, 70%, 80%, 90%, 95%) followed by two final incubations in 100% ethanol. Ethanol was removed by two incubations in hexamethyldisilazane. Samples were air-dried overnight under a fume hood. Subsequently, samples were placed on a stamp and sputter coated with gold. Finally, samples were imaged with a JEOL JCM 6000 benchtop SEM. Detailed information can be found in[57].

Mechanical testing

Uniaxial pulling tests were performed in a wet state for the different groups under a BOSE testing bench using fixed clamps. Sample length was set to 1 cm, while thickness and width were individually measured. Crosshead speed was set to 0.05 mm/s and pulling up to 0.9 strain. Elastic moduli were calculated as the slope of the most linear region presented on the stress over strain curve. Stress and strain were obtained in agreement with the initial cross sectional area and length of each sample.

Maximum stress was obtained as the maximum load before sample rupture. Detailed information can be found in[57].

Cell culture

All cell types were maintained at 37°C at 5% CO_2 and were negatively tested for mycoplasma contamination and cultured in their respective medium. Detailed information can be found in[57].
Murine HL-1 cardiomyocytes (HL-1) were generously provided by William C. Claycomb (Louisiana State University, New Orleans, LA, USA) and used at passages 18–44. Human cardiac fibroblasts (hCF; generously donated by S. van Linthout, BCRT, Berlin) and used at passage 7-10. Human immune cells (monocytes, macrophages and peripheral blood mononuclear cells) were isolated from Buffy Coat (obtained from Deutsches Rotes Kreuz, approved by the Institutional Review Board and ethics committee of Charité—Universitätsmedizin Berlin) using Biocoll density gradient. Monocytes were isolated from PMBCs using the CD14+ Magnetic Cell Separation kit. Macrophages were differentiated from isolated monocytes in the presence of M-CSF and collected with a cell scraper. Human EPDCs were isolated from human heart auricles as described [44] by peeling off the epicardial layer and trypsin/EDTA incubation. Adult human atrial samples (auricles) were obtained during cardiac surgery as redundant material anonymously collected under general informed consent. EMT was induced by addition of Transforming Growth Factor beta (TGF-β) for 7 days to cell culture medium. ICMPs were generated by forced expression of cardiac transcription factors in cardiac fibroblasts and kindly provided by Diphti Bachamanda-Somesh from our group (manuscript in preparation) were generated.

Simulated ischemia

Cells were cultured on patch materials or cell culture dishes for 24 h before being exposed to glucose/serum deprivation (glucose- and FBS-free DMEM supplemented with penicillin/streptomycin, 1% O2/5% CO2) for 5 h at 37°C.

Analyses of cell-scaffold interaction

Detailed information can be found in[57].
For determining adhesion rates, cells were labelled with Calcein, placed onto the patches and incubated at 37 °C for 30 min, 60 min, or 120 min. Supernatants containing unbound cells were collected and lysed. Fluorescence intensity, representing the number of cells, was analyzed using a Mithras LB940 plate reader and adherent cell number was calculated via comparison to a defined cell number standard.
Determination of cell necrosis was performed by measuring the release of Lactate Dehydrogenase (LDH). Here, cells were cultured for 24h under either normoxic conditions or simulated ischemia. Next, supernatants were analyzed for LDH release according to manufacturer's instructions, and fluorescence was measured using the Mithras LB940 plate reader. Results were normalized to normal cell culture conditions.
Cell growth was analyzed by measuring BrdU incorporation. To determine cell growth, cells were cultured under standard conditions for 24h. Subsequently, labelling reagent was added and incubated for 5h under normoxia or simulated ischemia. Afterwards, cells were analyzed for BrdU-incorporation according to manufacturer's protocol.
LIVE/DEAD Cell Viability Assay was performed following instructions from ThermoFisher Scientific.

Assessment of the immunological capacity of the scaffolds

Detailed information can be found in[57].
For flow cytometry analyses cells were collected and washed once. Then 50 µl staining solution comprised of antibodies was added and incubated for 30 min at 4°C. Subsequently, the suspension was washed and fixed with Paraformaldehyde (PFA) and analyzed the next day. The following antibodies were used for macrophage staining: CD163-Fitc, D80-PE, CD16-PerCPCy5.5, CD206-APC, CD14-APCCy7, HLA-DR-PeCy7, Life/Dead-V510. Antibodies for T cell proliferation: CD8-PE, CD4-APC, CD3-APCCy7.

To determine cytokine secretion, monocytes were cultured onto patch materials and incubated for 24h. As positive control, medium was supplemented with 200 ng/mL Lipopolysaccharide (LPS). Supernatants were collected and cytokine secretion was detected using ELISA technology for IL-6, IL-10 and TNF-α.
To investigate macrophage polarization, macrophages were cultured for 48h with or without the patches. To induce polarization towards M1, the culture medium was supplemented with Interferon gamma (INFy) and LPS. For M2a polarization, IL-4 and for M2c IL-10 was used. After 2 days of culture, supernatants were collected for detection of cytokine secretion via ELISA technology for IL-6, IL-10 and TNF-α. Cells were harvested using Accutase and analyzed for polarization marker expression by flow cytometry.
PBMCs (provided by Karen Bieback; Heidelberg as well as isolated from Buffy Coat) were stained with Carboxyfluorescein Succinimidyl Ester (CFSE) and cultured on patches for 5 days. The positive control medium was supplemented with Phytohaemagglutinin (PHA). Subsequently, cells were harvested and analyzed for proliferation of CD3+, CD3+/CD4+ and CD3+/CD8+ T cell proliferation by flow cytometry. Supernatants were collected and cytokine secretion was detected using ELISA technology for IL-6, IL-10 and TNF-α following the manufacturer's protocol.

Statistics

Data are shown as mean ± SEM. Comparisons passed normality and equal variance testing before the significance was tested. Differences between more than two groups were determined by one-way ANOVA with Bonferroni post-hoc for multiple comparisons. For two-group comparisons, a two-tailed student's t-test was performed if the normality test was passed. The Mann-Whitney test was performed if non-normality was detected. Changes over time were tested by two-way ANOVA with Bonferroni's correction. GraphPad Prism v. 5.03 (GraphPad, La Jolla, CA, USA) was used for data analysis and plotting. A p-value of $p < 0.05$ was considered significant.

RESULTS

The cytoprotective capacity of processed hcECM varies with pH during digestion

Previously, we could demonstrate that hcECM powder exerts a cytoprotective capacity on contractile cells *in vitro*. A similar effect was not observed when a homogenized ECM solution was produced by using a pepsin digestion at pH1 and 37°C for 48 h. However, a preservation of the cytoprotective capacity was achieved by changing the protocol to pH2 and room temperature resulting in a homogenized ECM solution after 48 h of digestion, with the ability to form a hydrogel (**Figure 1**)[59]. Both, ECM particles and the newly prepared hgECM exerted a clear cytoprotective effect by increasing the metabolic activity under ischemic conditions approximately by 1,5 fold[59].

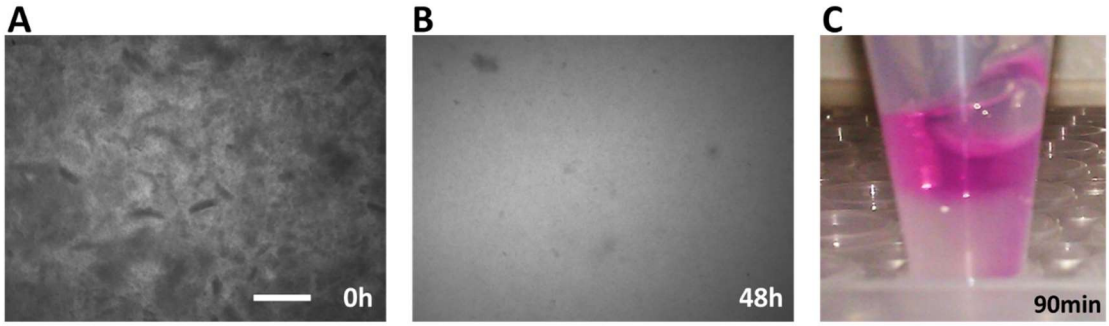

Figure 1: Pepsin based digestion of hcECM; A: Particles before digestions; B:homogenization of ECM particles within 48h results in hgECM solution; C: Self-assembling of hgECM solution within 90 min at 37°C. [modified from: Kappler, Benjamin, …, **Becker, Matthias** et al. 2016[59]]

Analysis by Mass Spectrometry identified 113 proteins in total within in the hgECM, of which 51 belong to the Extracellular Region Part. ECM proteins such as different types of collagen, dermatopontin, fibrillin 1 and fibronectin 1 were preserved[57], but interestingly, also a significant number of extracellular exosome associated proteins could be found in the hgECM. Altogether, the protocol not only preserves major ECM proteins but also a multitude of ECM exosome associated proteins and ultimately the cytoprotective function of the ECM[58]. The protocol is suitable for upscaling, GMP production or translation into the clinic.

HgECM allows uniformly patch coating without loss of scaffold stability

After establishing a protocol to homogenize ECM microparticles, the new hydrogel could completely cover a biological (DeAM) and polymeric (PEEU) scaffold material, resulting in novel scaffold materials DeAM+E and PEEU+E (**Figure 2**).

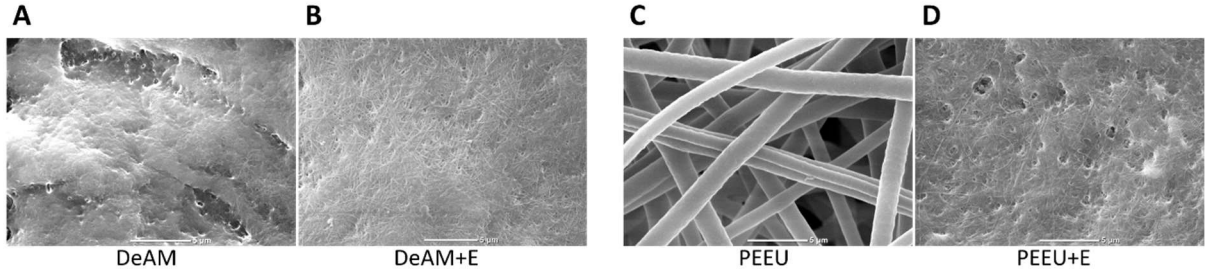

Figure 2: Different scaffolds coated with hgECM and visualized with scanning electron microscopy; DeAM (A, 5000x, scalebar 5 µm) and DeAM+E (B, 5000x, scalebar 5 µm), PEEU (C, 5000x, scalebar 5 µm) and PEEU+E (D, 5000x, scalebar 5 µm). [A, B: modified from **Becker, Matthias**, et al. 2018[57]; C, D: manuscript in preparation]

Due to their origin, the two materials strongly differ in their shape prior to coating. in both cases The additional hgECM coating covered the whole surface of both scaffolds and formed a solid uniform layer with the shape of nano-scaffold (**Figure 2** B and D).
Mechanical characteristics were tested by uniaxial pulling test (**Figure 3**) to evaluate a potential impact by scaffold coating. Mechanical analyses revealed different mechanical properties between the two materials. The polymeric materials turned out to be more flexible (**Figure 3** C and D) – lower E-Modulus – than the amniotic material (**Figure 3** A and B) but maximal stress resistance is higher for amniotic material[57]. The hgECM (DeAM+E, PEEU+E) coating did not affect any property of mechanical resistance.

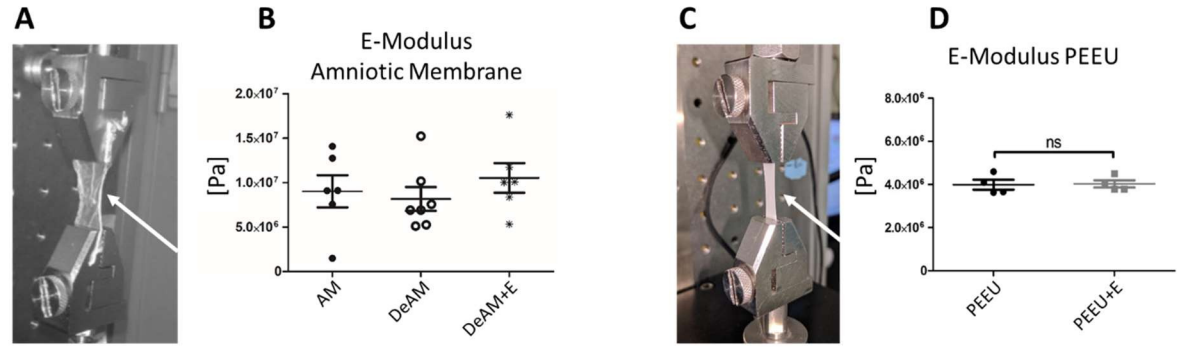

Figure 3: Mechanical testing of scaffold materials by uniaxial pulling test. Amniotic (A, arrow) and PEEU scaffolds (C, arrow) get clamped in the device and pulled in opposite directions until rupture to determine the Elastic Modulus. In case of amniotic tissue, native membrane (AM), DeAM and DeAM+E were tested (B). For polymeric scaffold, PEEU and PEEU+E were tested (D). [A, B: **Becker, Matthias**, et al. 2018 [57]; C, D: manuscript in preparation]

Coating with hgECM improves cell adhesion and viability

To examine the cardio- and cytoprotective influence of the hgECM coating, different cell types relevant for cardiac regeneration processes, namely human cardiac fibroblasts (hCFs), human EPDCs [57], and murine cardiomyocyte-like cells (HL-1, **Figure 4**) were cultured on the different scaffolds and adhesion capacity and viability was measured.

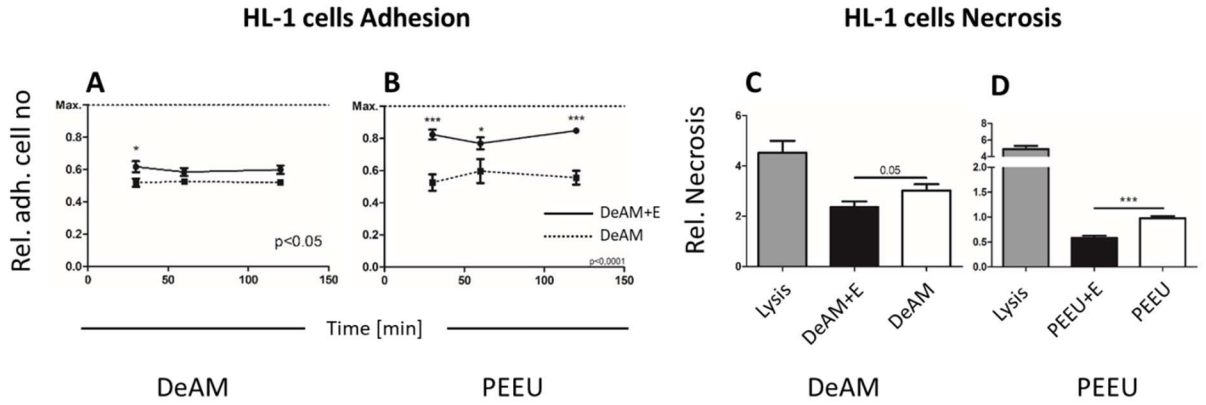

Figure 4: Interaction and viability of HL-1 cells with hgECM coated scaffolds. Cardiac cell (here HL-1 cells) were seeded on scaffold materials and adhesion capacity for DeAM (A) and PEEU (B) as well as cell necrosis for DeAM (C) and PEEU (D) were determined. A hgECM coating (DeAM+E, PEEU+E) improve adhesion capacity and reduces cell necrosis. * $p < 0.05$, ** $p < 0.01$, *** $p < 0.001$; $n \geq 3$. [A, C: **Becker, Matthias**, et al. 2018[57]; B, D: manuscript in preparation]

Both DeAM (**Figure 4**, A) and PEEU (**Figure 4**, B) showed improved HL-1 cell adhesion after coating. After hgECM coating a higher number of HL-1 cells were adherent on the scaffold. On DeAM scaffold only a slight improvement was observed. In contrast, the adhesion capacity on the PEEU scaffold was dramatically improved for HL-1 cells with hgECM coating compared to uncoated material (**Figure 4**, B). In addition, cell death of HL-1 cells was reduced on hgECM coated scaffolds (**Figure 4**, C and D). The same effect was observed when EPDCs and hCF were cultured on hgECM coated scaffolds [DeAM:[57]; PEEU: manuscript in preparation]. Moreover, a clear increase of proliferation by BrdU incorporation for all three cell types was observed after culturing on DeAM+E under normoxic and ischemic conditions[57]. Technical circumstances prohibited to perform a BrdU incorporation for PEEU. A live/dead staining was performed instead. Here, cells cultured on PEEU+E were found to be more vital than when cultured on PEEU without coating [PEEU: manuscript in preparation].

Bioactivity of epicardial patch system can be specifically enhanced by incorporating of cells relevant for cardiac regeneration

In addition to the general cardio- and cytoprotective capacity, we were interested in a way to further enhance bioactivity. Therefore, by transdifferentiation of cardiac fibroblasts, our group designed, produced and studied a new cardiac progenitor cell type (iCMPs). This cell line is characterized by the fact that first, it already shows the expression of cardiac markers and second, it has not yet lost its ability to proliferate [manuscript from our group in preparation]. They thereby present the optimal candidate to replace the defunct beating cells by proliferation rather than differentiation / maturation. Therefore, we investigated the compatibility of iCMPs with the scaffolds, with or without hgECM coating (**Figure 5**).

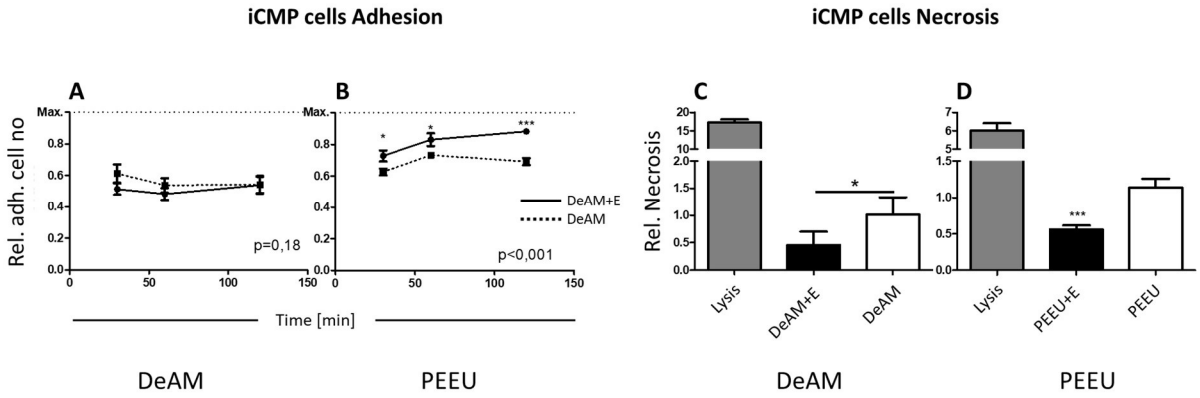

Figure 5: Co-Culture of induced cardiomyocytes progenitors (iCMPs), generated by transdifferentiation of cardiac fibroblasts, with scaffold materials and determination of adhesion capacity on DeAM (A) and PEEU (B) as well as cell necrosis on DeAM (C) and PEEU (D) under simulated ischemia conditions. * $p < 0.05$, ** $p < 0.01$, *** $p < 0.001$; $n \geq 3$. [All data: manuscript in preparation]

On amniotic scaffolds, a slightly better adhesion was observed with hgECM at 30 min, however, at 120 min no difference was observed between coated and uncoated scaffolds (**Figure 5** A). In contrast, on polymeric scaffolds adhesion was improved for all time points on PEEU+E (**Figure 5** B). In addition, for both scaffolds cell necrosis was reduced under simulated ischemia conditions with hgECM coating (**Figure 5** C, D) plus a higher proliferation rate was observed for DeAM+E[57]. Therefore, hgECM coating supports the adhesion and viability of iCMPs on biological and polymeric scaffolds.

Coating with hgECM modulates inflammatory responses

Inflammation and the balance between pro- and anti-inflammatory stimuli is critical in the healing process. It is important that any implant does not disturb the balance and should not be pro-inflammatory, i.e. activate 'foreign body response' to exert desired regenerative effects. The secretion of IL-6 (**Figure 6**) as well as TNF-α and IL-10[57] by monocytes on hgECM coated and non-coated scaffolds were measured to determine immunological potential of the scaffolds. In addition, secretion of IL-6, TNF-α and IL-10 of macrophages and PBMCs were measured upon scaffold interaction. Additionally, macrophage polarization and T cell proliferation were determined by flow cytometry [DeAM: [57]; PEEU: manuscript in preparation].

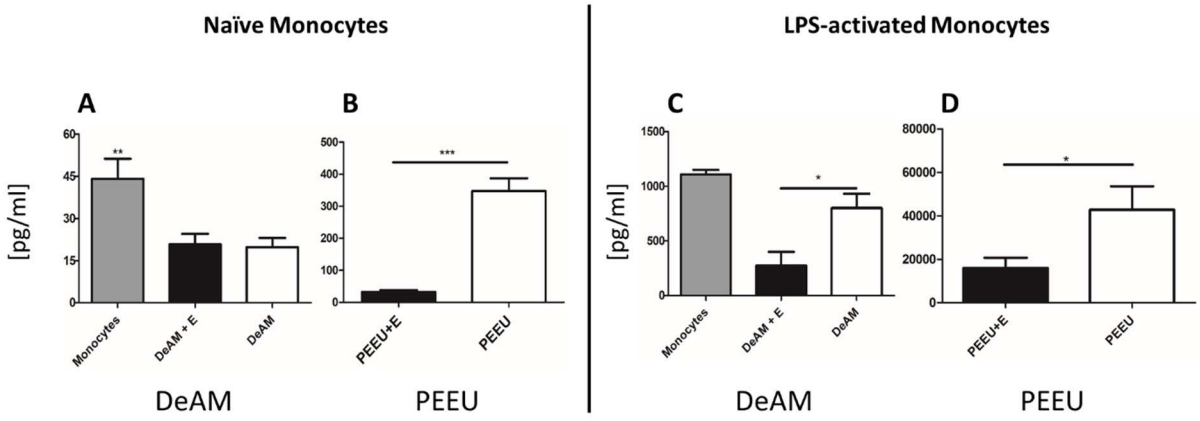

Figure 6: Pro-inflammatory cytokine release (IL-6) from naïve monocytes cultured on DeAM (A) or PEEU (B) from LPS-activated monocytes cultured on DeAM (C) or PEEU (D). A hgECM coating reduces pro-inflammatory cytokine secretion by LPS activated monocytes upon contact with both scaffolds and by naïve monocytes on PEEU scaffold. * $p < 0.05$, ** $p < 0.01$, *** $p < 0.001$; $n \geq 3$.[A, C: **Becker, Matthias**, et al. 2018 [57]; B, D: manuscript in preparation]

Secretion of pro-inflammatory cytokines, such as IL-6, was clearly reduced by LPS-activated monocytes upon contact with both scaffolds coated with hgECM (**Figure 6** C, D). On amniotic scaffolds, hgECM

coating had no effect on secreted levels of IL-6 by naïve monocytes. However, secretion levels were still significantly less than by naïve monocytes on standard culture plate (**Figure 6** A). Interestingly, non-stimulated monocytes secrete significantly more IL-6 when cultured on PEEU, whereas hgECM coating diminished that effect (**Figure 6** B). The same observation was done for TNF-α. In contrast, the secretion of IL-10 was not affected. Macrophages and PMBCs showed no difference in cytokine secretion between hgECM coated and non-coated scaffolds. Moreover, analyses of surface marker expression by flow cytometry did not reveal a pro-inflammatory macrophage polarization and T cell proliferation[57]. In summary, hgECM coating caused a shift of the scaffolds towards a more anti-inflammatory effect.

Polymorph nuclear cells allow a faster prediction of innate inflammatory responses in future

To establish a rapid analysis for potential inflammatory responses of implants, a study focusing on PMNs was started in cooperation with Maria Schneider from the Institute of Medical Immunology, Charité-Universitätsmedizin Berlin, and its functionality was established by using the amniotic material as a "proof-of-principle" implant. PMNs are the most abundant leukocytes in blood and the first players in immune reactions. Thus, they highlight the initial and therefore fastest cellular response upon transplantation. As many studies evaluate the immunogenicity of an implant material dealing with the behavior of macrophages or T cells[60–62], a deeper focus on PMNs activation upon biomaterial contact is needed to predict the outcome of new implant strategies. We therefore established an *in vitro* activation strategy of PMNs and analyzed the PMN/implant interaction (**Figure 7**).

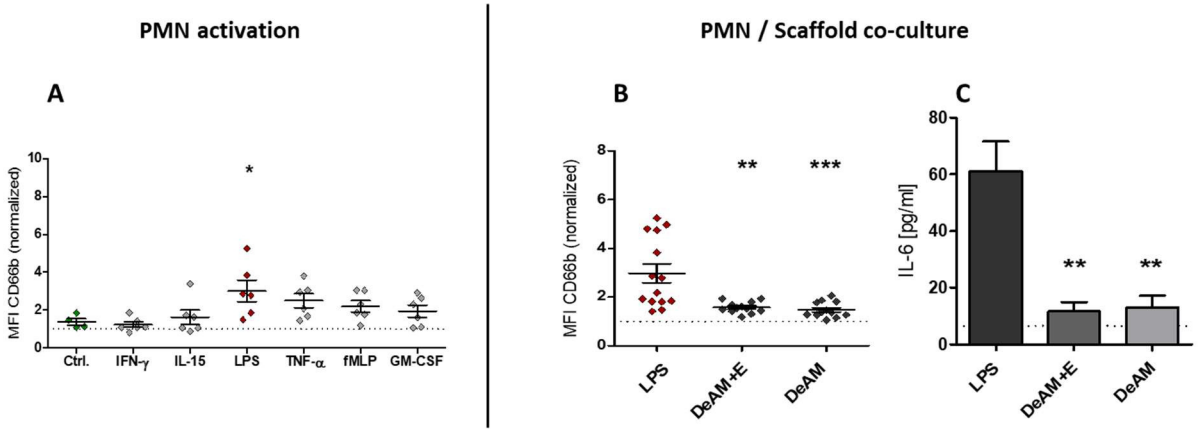

Figure 7: PMN activation and co-culture on ECM scaffolds. A multi-comparison analysis of different *in vitro* activation strategies identified LPS as most effective pro-inflammatory stimulator (A). Co-culturing on a trial basis on amniotic scaffolds revealed no activation of PMNs, neither on surface marker expression (B), nor on pro-inflammatory cytokine secretion (C). * $p < 0.05$, ** $p < 0.01$, *** $p < 0.001$; $n \geq 3$. [All data: manuscript in preparation]

Comparing different published activation strategies, pro-inflammatory activation by LPS was found to be most effective for PMN-activation (**Figure 7** A). In co-culture with hgECM coated biological scaffolds (DeAM / DeAM+E), no activation was observed, neither via cell surface marker expression (**Figure 7** B) nor pro-inflammatory cytokine release (IL-6, **Figure 7** C). Therefore, a suitable strategy for *in vitro* analyses was identified and successfully applied on the first biological implant scaffold material. The potential for future applications to apply this technique to other implantable materials is thereby demonstrated.

DISCUSSION

The regenerative potential of the heart is insufficient for complete repair after an MI. Studies so far have researched the potential of ECM and epicardial patches in cardiac regeneration, but have not been translated to the clinic yet. In the present work, I demonstrate that ECM isolated from human

myocardium has the potential to modify the regenerative properties of a scaffold with a biological or polymeric nature, thereby increasing its suitability for therapeutic applications in the infarcted and failing heart.

Processing of human cardiac ECM preserved its protein content and cytopretective capacity

ECM is a vital component for cardiac regeneration. It plays not only an essential role in cardiac remodeling after MI, but also in pathologies that lead to heart failure[63] and influences cellular differentiation due to its specific multi-protein composition and 3D architecture [64]. Therefore, cardiac ECM has been isolated from a variety of species with the focus on the regenerative capabilities of ECM in cardiac applications [65–68]. Research has shown it has anti-inflammatory potential and the ability to induce specific gene expression [54,69–72]. The preservation of regenerative potential after processing to microparticles or hydrogel was even observed in large animals after intramyocardial injection[48,52,73]. Regardless of all the observed successes, the regenerative effects so far were only observed with (cardiac) ECM of animal origin applied in an animal infarction model. Considering a clinical translation, the source of ECM should ideally be human, due to the species-specific composition of the cardiac ECM[56]. The possibilities of applying human material have been less thoroughly researched. A first attempt to design a patch consisting of human ECM slices only worked by fibrin-stabilizing[74] and a loss of GAGs[75]. Furthermore, the size of original human cardiac tissue and the very fragile composition of the ECM slices limited the application range and emphasize the need for a homogenization step.

Processing of human cardiac ECM has not been researched before. Therefore, we established a homogenization protocol to obtain hcECM hydrogel. Published protocols were mainly using Pepsin based digestion procedures but are varying in the precise protocols[76–78]. This procedure theoretically could be also applied for human cardiac tissue but there is only a vague orientation in the literature about the right parameters, partially even contradicting with the manufacturer's recommendations. Pepsin is an amide-bond endopeptidase that requires optimal working conditions of pH2 and up to 42°C[79] – an environment that directly influences the ECM peptide composition, thereby potentially influencing the biologic activity of the pepsin and ultimately affecting the biologic activity of the hgECM. Thus, only a precise parameter-adjustment balances uniformly homogenization and preservation of proteins relevant for cyto- and cardioprotection. Our first attempt using a digestion at pH1 for 48h at 37°C was not successful[59]. Adjusting these parameters to pH2 for 48h at 27°C resulted in a standardized protocol to homogenize the hcECM with preservation of the cytoprotective properties of hgECM[58]. For subsequently scaffold coating 8mg/ml was chosen as it was identified as a therapeutically relevant concentration[73,77].

The unique composition of the cardiac ECM contributes to its pro-regenerative properties. Thus, the preservation of its contents after processing are vital for its use in any therapeutic applications. Previous studies with ECM hydrogels only identified a short list of ECM proteins[56] with typical ECM proteins outnumbered. Our analysis of the hgECM with mass spectrometry identified ECM/extracellular proteins as well, responsible for cell adhesion, different metabolic processes or viability. Interestingly, besides cellular and extracellular components, a large number of proteins associated to ECM exosomes were found. Regarding regeneration, extracellular vesicles represent a novel component known to be beneficial in different contexts of regenerative attempts and they are known to contain several beneficial proteins and micro-RNAs (miR)[80–84]. As cells are surrounded by ECM, it was a logical consequence that biologically active matrix bound vesicles (MBV) were found[85,86] and different miRs were suspected to be responsible for observed regenerative effects. The existence of intact vesicles in hydrogels is not described as it is unlikely to have remained intact due to the very acidic pepsin based digestion step destructive for vesicles[87]. Interestingly, by mass spectrometry we identified proteins associated to extracellular exosomes. Thus, the cytoprotective effects of hgECM could be explained by proteins from the extracellular vesicles as well. In depth analysis is needed to confirm the presence of

either preserved miRs or even intact vesicles within the hgECM and potentially identify a relevant biological compound to give a deeper explanation for the protective capacity of hgECM.

A hgECM coating of scaffolds increase cardiac compatibility

The application of epicardial scaffolds provide, in contrast to intramyocardial injection strategies, a controlled local treatment and support the activated epicardium after MI. Furthermore, patches provide the opportunity to implement a plethora of bioactive enhancers, such as cells or cytokines.

We pursued two strategies to design a novel cardiac patch system, biological and polymeric respectively. The biological patch consisted of DeAM as an ECM scaffold with known regenerative potential[88–91], which, in its uncoated form, we previously tested successfully *in vivo* in a murine infarction model[41]. Therefore, we already established the regenerative potential of the DeAM, which is in corroboration with other studies identifying the regenerative potential of different ECM scaffolds [85]. For this material, a GMP-based upscaling is only possible within limits, as its availability is dependent on human material (placenta). Therefore, we also tested a polymeric patch, namely an electro spun PEEU scaffold eliminating the disadvantage of the amniotic membrane. Here, upscaling is easily possible due to the standardized electro spinning technique, but the biological function is limited, since only small adjustments are possible in fiber composition [31,34]. To compensate that disadvantage, in the past proteins were integrated to make a polymer more biological compatible. Until now only single proteins, such as gelatin [29], fibrin [92] and collagen[93] were used. However, even incorporating these mentioned single proteins, the patches still do not provide organ specificity. If easily achievable porcine cardiac ECM is aimed to add organ specific proteins, a comparison of human and porcine cardiac ECM revealed a divergent protein composition[56] potentially having consequences for the application in humans in future clinical translation. Therefore, only incorporating human cardiac ECM provides a variety of organ-specific bioactivity and represents the only attempt to achieve the maximal clinical success in the future.

After homogenizing of the ECM[58], a dry-coating protocol[94] was chosen to facilitate the combination of the scaffolds with human cardiac ECM. Firstly, to avoid dramatically influence of the mechanical properties of the polymer[95] and, secondly, to guarantee a similar treatment of both scaffolds as for DeAM only a dry-coating protocol allows scaffold/ECM combination. It rather allows future translation to a variety of other implants than incorporation in a spinning process.

We measured the mechanical properties and although both scaffold materials met the minimal criteria [30] to allow epicardial application, their mechanical behaviors were different. Artificial polymer materials generally show a rather linear mechanical behavior[96], as well as we observed, while the natural flexibility of the amniotic membrane allows for some compensation of the applied stress[57]. As material stiffness can have a significant impact on cell behavior[97,98], these different behaviors can reveal a different regenerative potential in the complex beating system later on. But in line with our strategy for scaffold/ECM combination, we did not observe a difference in the mechanical properties of coated and uncoated scaffolds.

An epicardial patch must hold a certain cytoprotectivity with focus on cardiac cells, which is most likely determined by its tissue-specific protein composition[43]. As a general observation of cell-scaffold interaction have not been made, a prediction about the cellular response to our scaffolds were impossible and so we investigated the biologic activity of the myocardial ECM product regarding cardio protection. The hgECM coating caused a smoother surface with a smaller fiber size. Considering the variety of scaffold designs modifying the fiber composition and arrangement, scaffold surfaces appear in principle not different to generally published attempts[99]. Even though similar polymer materials have been shown to be biocompatible, we show here that adhesion of HL-1 cells (and EPDCs[57]) improved upon coating with hgECM. This difference can be explained by the fact that the hgECM contains several proteins beneficial for cell adhesion. For example, fibronectin was found in the hgECM and is part of the standard cell coating for HL-1 cells[100]. Also, the improved viability of contractile HL-1 cells and EPDCs demonstrate the fundamentally improved biocompatibility of the PEEU scaffold but also the beneficial shift of regenerative properties of DeAM upon hgECM coating.

Inflammatory response is reduced by hgECM coated scaffolds

Inflammation is a highly relevant process of a cardiac infarction[101]. Timely resolution of inflammation is key to a normal healing process. An imbalanced pro-inflammatory situation can disturb and worsen healing processes, holding the risk to dramatically decrease cardiac function or even death. It has been shown that electro spun polymer can induce pro-inflammatory macrophage polarization towards M1-type, [37] whereas introduction of collagen or ECM can reverse the polarization towards anti-inflammatory M2 type [69–71,102]. On our scaffolds we have observed similar effects in monocyte cytokine secretion. On amniotic scaffolds, the additional coating with hgECM reduced pro-inflammatory cytokine secretion upon LPS-activation. In contrast, PEEU coated with ECM reduced not only secretion of pro-inflammatory cytokines upon LPS activation, but also the secretion from naïve monocytes. Most likely PCL, a part of PEEU, causes the pro-inflammatory reaction [37] and collagen has been shown to be able to reverse that effect. Since collagen is included in the hgECM, our findings are in corroboration with these results. The PEEU polymer is a co-block polymer and consists not only of PCL but also of Dioxanone. That may explain the diminished effect on macrophages on PEEU meaning no observed pro-inflammatory macrophage reaction (i.e., M1 polarization). However, the presence of ECM can counteract the pro-inflammatory effects of uncoated scaffolds[73]. Therefore, according to our expectations scaffolds containing ECM (PEEU+E and both amniotic scaffolds) did certainly not induce a M1 polarization but rather tend to induce a polarization towards the anti-inflammatory M2-type[57]. Moreover, Ariganello et al.[103] highlights in particular decellularized pericardial tissue being supportive for guiding macrophage polarization towards anti-inflammatory tissue-remodeling state, underlining the beneficial impact of ECM coating with human cardiac background especially for polymer scaffolds.

In addition, while M1 polarization was not observed on PEEU scaffolds, the majority of macrophages cultured on PEEU had to be gated as cell debris. Thus, PEEU does not support the viability of macrophages, similar to the results with cardiac cells. In contrast, the PEEU+E not only preserved the viability of macrophages crucial for remodeling processes of the infarcted myocardium [104], but also prevented macrophages from polarization towards M1-Typ.

Macrophages on DeAM were not activated, as expected for macrophages cultured on an ECM material. As both DeAM and DeAM+E consists of ECM, neither an obvious cell death nor an M1 polarization was observed. Again, this is in line with the findings that ECM proteins, such as collagen – an element of DeAM as well as hgECM – support cellular viability and has a rather anti-inflammatory potential.

In line with an immune reaction, PMNs represent the very first player and are essential to orchestrate the immunological behavior of ensuing immune cells, e.g. monocytes. So, they immediately interact with implanted matrices[105]. In contrast to well-established *in vitro* assays dealing with monocytes, macrophages or T cells[106], PMNs are separately analyzed either in clinical cases such as Gingivitis, Chlamydia infection and neuronal diseases[107–111] or in *in vitro* PMN-activation strategies with various outcome[112–117]. As there is a gap between clinical observations and *in vitro* measurements, we applied published *in vitro* PMN-activation strategies on PMNs. We isolated PMNs from peripheral blood from arm vein blood, as it represents a neutral and common cell source for subsequent standardized protocols. We identified only LPS as an effective activator for PMNs. For a translational analysis, PMNs were co-cultured with amniotic scaffolds as a "proof-of-principle" material. The fact that no pro-inflammatory activation of PMNs was observed, matches with our previous observations about the inflammatory cells on amniotic scaffolds. This newly established technique represents not only a comparative study how to activate PMNs and an easy and suitable assay to evaluate PMN response to biological matrices *in vitro* but also a faster way compared to established tests with monocytes, or macrophages to predict the immunogenicity and compatibility of the material later on *in vivo*. In short term, the immunological behavior of the PEEU scaffolds can be approached. In the long term, this assay can be applied to any future implant as well.

Future clinical application of epicardial scaffolds facilitates new cardiac regeneration strategies

In the future we aim at applying the hgECM coated composite materials to the activated epicardial surface of the infarcted human heart, since the epicardium is highly involved in cardiac regeneration processes [118]. The materials will provide an optimal carrier system for local and controlled delivery of biomaterial as well as bioactive compounds.

The patch systems were biologically enhanced by colonialization of iCMPs, designed and generated in our group from CFs by transdifferentiation. In contrast to fully differentiated cardiomyocytes derived from induced pluripotent stem cells (iPS), iCMPs still have the ability to proliferate – an ability almost lost in cardiomyocytes[5]. Therefore, iCMPs hold the advantage that the number of cells needed to provide a clinical relevant effect is reduced compared to iPS derived cardiomyocytes, as they cannot proliferate anymore. By providing proliferating iCMPs with the potential to differentiate towards mature cardiomyocytes, the infarcted region is optimally supported by a passive bioactive compound (hgECM) combined with an active bioactive compound (iCMP). Even though iCMPs need to migrate from the epicardium into the myocardium to replace lost cardiomyocytes, they can support the disrupted infarct zone by paracrine stimulation epicardially as well as finally myocardially.

So far it remains unclear how cECM precisely exerts its cytoprotective effects. However, the addition of a complex mix of organ specific proteins undoubtedly incorporates an optimal ground for cellular interaction and supports the objective that coating of scaffold materials increases cell proliferation and reduces cell necrosis as well as pro-inflammatory cytokine secretion. Furthermore, the combination of coated scaffolds with iCMPs theoretically provides the optimal combination to specifically support the weakened heart. The limited regenerative capacity of the human heart can be strengthened by a designed epicardial patch design presented here.

In conclusion, epicardial hybrid patch systems were tailored for cardiac regeneration after MI. The patch system specifically supports viability of cardiac cells and holds the potential to epicardially transfer regeneratively potent iCMP cells. *In vivo* analyses in a myocardial infarction model ultimately will reveal the regenerative potential in a complex system. In the clinical future of cardiac regeneration, the presented epicardial patch system is first of all an easy treatment strategy as it only requires opening the pericardium followed by a basic suturing. However, while intramycardial treatments can be applied minimally invasive by catheter, epicardial treatments most likely requires a thoracotomy. That represents a very severe invasive intervention and huge stress for the patient. It remains a challenging but solvable mission to evolve surgical methods to reduce stress for the patient and still successfully apply the epicardial patch.

With focus on clinical application, the used hgECM provides optimal organ and species specific regenerative bioactivity and the colonized iCMPs represent a potent enhancement to replace lost cardiomyocytes. Altogether, the epicardial patch system presented here has the potential to improve cardiac remodeling and function after myocardial infarction in future clinical applications.

BIBLIOGRAPHY

1. Roger, V. L.; Go, A. S.; Lloyd-Jones, D. M.; Benjamin, E. J.; Berry, J. D.; Borden, W. B.; Bravata, D. M.; Dai, S.; Ford, E. S.; Fox, C. S.; Fullerton, H. J.; Gillespie, C.; Hailpern, S. M.; Heit, J. A.; Howard, V. J.; Kissela, B. M.; Kittner, S. J.; Lackland, D. T.; Lichtman, J. H.; Lisabeth, L. D.; Makuc, D. M.; Marcus, G. M.; Marelli, A.; Matchar, D. B.; Moy, C. S.; Mozaffarian, D.; Mussolino, M. E.; Nichol, G.; Paynter, N. P.; Soliman, E. Z.; Sorlie, P. D.; Sotoodehnia, N.; Turan, T. N.; Virani, S. S.; Wong, N. D.; Woo, D.; Turner, M. B.; American Heart Association Statistics, C.; Stroke Statistics, S. Heart disease and stroke statistics--2012 update: a report from the American Heart Association. *Circulation* **2012**, *125*, e2–e220 10.1161/CIR.0b013e31823ac046.
2. Nichols, M.; Townsend, N.; Scarborough, P.; Rayner, M. Cardiovascular disease in Europe 2014: epidemiological update. *Eur. Heart J.* **2014**, *35*, 2950–2959 10.1093/eurheartj/ehu299.
3. Langone, A. J.; Helderman, J. H. Disparity between solid-organ supply and demand. *N Engl J Med* **2003**, *349*, 704–706 10.1056/NEJMe038117.
4. Bergmann, O.; Bhardwaj, R. D.; Bernard, S.; Zdunek, S.; Barnabé-Heide, F.; Walsh, S.; Zupicich, J.; Alkass, K.; Buchholz, B. A.; Druid, H.; Jovinge, S.; Frisén, J. Evidence for cardiomyocyte renewal in humans. *Science (80-.).* **2009** 10.1126/science.1164680, DOI 10.1126/science.1164680.
5. Mollova, M.; Bersell, K.; Walsh, S.; Savla, J.; Das, L. T.; Park, S.-Y.; Silberstein, L. E.; Dos Remedios, C. G.; Graham, D.; Colan, S.; Kühn, B. Cardiomyocyte proliferation contributes to heart growth in young humans. *Proc. Natl. Acad. Sci. U. S. A.* **2013**, *110*, 1446–51 10.1073/pnas.1214608110.
6. Porrello, E. R.; Mahmoud, A. I.; Simpson, E.; Hill, J. A.; Richardson, J. A.; Olson, E. N.; Sadek, H. A. Transient regenerative

potential of the neonatal mouse heart. *Science (80-.).* **2011**, *331*, 1078–1080 10.1126/science.1200708.
7. Vagnozzi, R. J.; Molkentin, J. D.; Houser, S. R. New Myocyte Formation in the Adult Heart. *Circ. Res.* **2018**, *123*, 159–176 10.1161/CIRCRESAHA.118.311208.
8. Van de Werf, F.; Bax, J.; Betriu, A.; Blomstrom-Lundqvist, C.; Crea, F.; Falk, V.; Filippatos, G.; Fox, K.; Huber, K.; Kastrati, A.; Rosengren, A.; Steg, P. G.; Tubaro, M.; Verheugt, F.; Weidinger, F.; Weis, M.; Vahanian, A.; Camm, J.; De Caterina, R.; Dean, V.; Dickstein, K.; Filippatos, G.; Funck-Brentano, C.; Hellemans, I.; Kristensen, S. D.; McGregor, K.; Sechtem, U.; Silber, S.; Tendera, M.; Widimsky, P.; Zamorano, J. L.; Silber, S.; Aguirre, F. V.; Al-Attar, N.; Alegria, E.; Andreotti, F.; Benzer, W.; Breithardt, O.; Danchin, N.; Mario, C. Di; Dudek, D.; Gulba, D.; Halvorsen, S.; Kaufmann, P.; Kornowski, R.; Lip, G. Y. H.; Rutten, F. Management of acute myocardial infarction in patients presenting with persistent ST-segment elevation. *Eur. Heart J.* **2008**, *29*, 2909–2945 10.1093/eurheartj/ehn416.
9. Prabhu, S. D.; Frangogiannis, N. G. The Biological Basis for Cardiac Repair After Myocardial Infarction. *Circ. Res.* **2016**, *119*, 91–112 10.1161/CIRCRESAHA.116.303577.
10. Dewald, O.; Ren, G.; Duerr, G. D.; Zoerlein, M.; Klemm, C.; Gersch, C.; Tincey, S.; Michael, L. H.; Entman, M. L.; Frangogiannis, N. G. Of mice and dogs: species-specific differences in the inflammatory response following myocardial infarction. *Am. J. Pathol.* **2004**, *164*, 665–77 10.1016/S0002-9440(10)63154-9.
11. Troidl, C.; Möllmann, H.; Nef, H.; Masseli, F.; Voss, S.; Szardien, S.; Willmer, M.; Rolf, A.; Rixe, J.; Troidl, K.; Kostin, S.; Hamm, C.; Elsässer, A. Classically and alternatively activated macrophages contribute to tissue remodelling after myocardial infarction. *J. Cell. Mol. Med.* **2009**, *13*, 3485–3496 10.1111/j.1582-4934.2009.00707.x.
12. Bader, A. M.; Brodarac, A.; Klose, K.; Bieback, K.; Choi, Y.-H.; Kurtz, A.; Stamm, C. Mechanisms of paracrine cardioprotection by cord blood mesenchymal stromal cells. *Eur. J. Cardio-Thoracic Surg.* **2014**, *45*, 983–992 10.1093/ejcts/ezt576.
13. Hastings, C. L.; Roche, E. T.; Ruiz-Hernandez, E.; Schenke-Layland, K.; Walsh, C. J.; Duffy, G. P. Drug and cell delivery for cardiac regeneration. *Adv. Drug Deliv. Rev.* **2015**, *84*, 85–106 10.1016/j.addr.2014.08.006.
14. Kuliszewski, M. A.; Fujii, H.; Liao, C.; Smith, A. H.; Xie, A.; Lindner, J. R.; Leong-Poi, H. Molecular imaging of endothelial progenitor cell engraftment using contrast-enhanced ultrasound and targeted microbubbles. *Cardiovasc. Res.* **2009**, *83*, 653–662 10.1093/cvr/cvp218.
15. Smith, R. R.; Marbán, E.; Marbán, L. Enhancing retention and efficacy of cardiosphere-derived cells administered after myocardial infarction using a hyaluronan-gelatin hydrogel. *Biomatter* **2013**, *3*, e24490 10.4161/biom.24490.
16. Masumoto, H.; Ikuno, T.; Takeda, M.; Fukushima, H.; Marui, A.; Katayama, S.; Shimizu, T.; Ikeda, T.; Okano, T.; Sakata, R.; Yamashita, J. K. Human iPS cell-engineered cardiac tissue sheets with cardiomyocytes and vascular cells for cardiac regeneration. *Sci. Rep.* **2015**, *4*, 6716 10.1038/srep06716.
17. Zhang, X.; Wang, H.; Ma, X.; Adila, A.; Wang, B.; Liu, F.; Chen, B.; Wang, C.; Ma, Y. Preservation of the cardiac function in infarcted rat hearts by the transplantation of adipose-derived stem cells with injectable fibrin scaffolds. *Exp. Biol. Med.* **2010**, *235*, 1505–1515 10.1258/ebm.2010.010175.
18. Dai, W.; Wold, L. E.; Dow, J. S.; Kloner, R. A. Thickening of the infarcted wall by collagen injection improves left ventricular function in rats: a novel approach to preserve cardiac function after myocardial infarction. *J Am Coll Cardiol* **2005**, *46*, 714–719 10.1016/j.jacc.2005.04.056.
19. Simpson, D.; Liu, H.; Fan, T. H.; Nerem, R.; Dudley Jr., S. C. A tissue engineering approach to progenitor cell delivery results in significant cell engraftment and improved myocardial remodeling. *Stem Cells* **2007**, *25*, 2350–2357 10.1634/stemcells.2007-0132.
20. van Wijk, B.; Gunst, Q. D.; Moorman, A. F. M.; van den Hoff, M. J. B. Cardiac Regeneration from Activated Epicardium. *PLoS One* **2012**, *7*, e44692 10.1371/journal.pone.0044692.
21. Masters, M.; Riley, P. R. The epicardium signals the way towards heart regeneration. *Stem Cell Res.* **2014** 10.1016/j.scr.2014.04.007, DOI 10.1016/j.scr.2014.04.007.
22. Lien, C. L.; Schebesta, M.; Makino, S.; Weber, G. J.; Keating, M. T. Gene expression analysis of zebrafish heart regeneration. *PLoS Biol.* **2006** 10.1371/journal.pbio.0040260, DOI 10.1371/journal.pbio.0040260.
23. Bock-Marquette, I.; Saxena, A.; White, M. D.; Michael DiMaio, J.; Srivastava, D. Thymosin β4 activates integrin-linked kinase and promotes cardiac cell migration, survival and cardiac repair. *Nature* **2004**, *432*, 466–472 10.1038/nature03000.
24. Bock-Marquette, I.; Shrivastava, S.; Pipes, G. C. T.; Thatcher, J. E.; Blystone, A.; Shelton, J. M.; Galindo, C. L.; Melegh, B.; Srivastava, D.; Olson, E. N.; DiMaio, J. M. Thymosin β4 mediated PKC activation is essential to initiate the embryonic coronary developmental program and epicardial progenitor cell activation in adult mice in vivo. *J. Mol. Cell. Cardiol.* **2009**, *46*, 728–738 10.1016/J.YJMCC.2009.01.017.
25. SMART, N.; RISEBRO, C. A.; MELVILLE, A. A. D.; MOSES, K.; SCHWARTZ, R. J.; CHIEN, K. R.; RILEY, P. R. Thymosin beta-4 Is Essential for Coronary Vessel Development and Promotes Neovascularization via Adult Epicardium. *Ann. N. Y. Acad. Sci.* **2007**, *1112*, 171–188 10.1196/annals.1415.000.
26. Rui, L.; Yu, N.; Hong, L.; Feng, H.; Chunyong, H.; Jian, M.; Zhe, Z.; Shengshou, H. Extending the time window of mammalian heart regeneration by thymosin beta 4. *J. Cell. Mol. Med.* **2014** 10.1111/jcmm.12421, DOI 10.1111/jcmm.12421.
27. van Tuyn, J.; Atsma, D. E.; Winter, E. M.; van der Velde-van Dijke, I.; Pijnappels, D. A.; Bax, N. A.; Knaan-Shanzer, S.; Gittenberger-de Groot, A. C.; Poelmann, R. E.; van der Laarse, A.; van der Wall, E. E.; Schalij, M. J.; de Vries, A. A. Epicardial cells of human adults can undergo an epithelial-to-mesenchymal transition and obtain characteristics of smooth muscle cells in vitro. *Stem Cells* **2007**, *25*, 271–278 10.1634/stemcells.2006-0366.
28. Zhou, B.; Honor, L. B.; He, H.; Ma, Q.; Oh, J.-H.; Butterfield, C.; Lin, R.-Z.; Melero-Martin, J. M.; Dolmatova, E.; Duffy, H. S.; Gise, A. von; Zhou, P.; Hu, Y. W.; Wang, G.; Zhang, B.; Wang, L.; Hall, J. L.; Moses, M. A.; McGowan, F. X.; Pu, W. T. Adult mouse epicardium modulates myocardial injury by secreting paracrine factors. *J. Clin. Invest.* **2011**, *121*, 1894–904 10.1172/JCI45529.
29. Prabhakaran, M. P.; Kai, D.; Ghasemi-Mobarakeh, L.; Ramakrishna, S. Electrospun biocomposite nanofibrous patch for cardiac tissue engineering. *Biomed Mater* **2011**, *6*, 55001 10.1088/1748-6041/6/5/055001.
30. Chen, Q.-Z.; Bismarck, A.; Hansen, U.; Junaid, S.; Tran, M. Q.; Harding, S. E.; Ali, N. N.; Boccaccini, A. R. Characterisation of a soft elastomer poly(glycerol sebacate) designed to match the mechanical properties of myocardial tissue. *Biomaterials* **2008**, *29*, 47–57 10.1016/J.BIOMATERIALS.2007.09.010.
31. Rüder, C.; Sauter, T.; Kratz, K.; Haase, T.; Peter, J.; Jung, F.; Lendlein, A.; Zohlnhöfer, D. Influence of fibre diameter and orientation of electrospun copolyetheresterurethanes on smooth muscle and endothelial cell behaviour. *Clin. Hemorheol. Microcirc.* **2013**, *55*, 513–522 10.3233/CH-131787.
32. Shayanti Mukherjee Rajeswari Ravichandran Seeram Ramakrishna Michael Raghunath, J. R. V. Evaluation of the Biocompatibility of PLACL/Collagen Nanostructured Matrices with Cardiomyocytes as a Model for the Regeneration of Infarcted Myocardium. *Adv Funct Mater* **2011**.
33. Kratz, K.; Habermann, R.; Becker, T.; Richau, K.; Lendlein, A. Shape-memory properties and degradation behavior of multifunctional electro-spun scaffolds. *Int J Artif Organs* **2011**, *34*, 225–230.
34. Ruder, C.; Sauter, T.; Becker, T.; Kratz, K.; Hiebl, B.; Jung, F.; Lendlein, A.; Zohlnhofer, D. Viability, proliferation and adhesion of

smooth muscle cells and human umbilical vein endothelial cells on electrospun polymer scaffolds. *Clin Hemorheol Microcirc* **2012**, *50*, 101–112 10.3233/CH-2011-1447.
35. Hiebl, B.; Mrowietz, C.; Goers, J.; Bahramsoltani, M.; Plendl, J.; Kratz, K.; Lendlein, A.; Jung, F. In vivo evaluation of the angiogenic effects of the multiblock copolymer PDC using the hen's egg chorioallantoic membrane test. *Clin. Hemorheol. Microcirc.* **2010**, *46*, 233–238 10.3233/CH-2010-1350.
36. Shin, M.; Ishii, O.; Sueda, T.; Vacanti, J. P. Contractile cardiac grafts using a novel nanofibrous mesh. *Biomaterials* **2004**, *25*, 3717–3723 10.1016/j.biomaterials.2003.10.055.
37. Castellano, D.; Blanes, M.; Marco, B.; Cerrada, I.; Ruiz-Sauri, A.; Pelacho, B.; Arana, M.; Montero, J. A.; Cambra, V.; Prosper, F.; Sepulveda, P. A comparison of electrospun polymers reveals poly(3-hydroxybutyrate) fiber as a superior scaffold for cardiac repair. *Stem Cells Dev* **2014**, *23*, 1479–1490 10.1089/scd.2013.0578.
38. Clare, G.; Suleman, H.; Bunce, C.; Dua, H. Amniotic membrane transplantation for acute ocular burns. *Cochrane Database Syst. Rev.* **2012** 10.1002/14651858.CD009379.pub2, DOI 10.1002/14651858.CD009379.pub2.
39. Bose, B. Burn wound dressing with human amniotic membrane. *Ann. R. Coll. Surg. Engl.* **1979**, *61*, 444–7.
40. Shun, A.; Ramsey-Stewart, G. Human amnion in the treatment of chronic ulceration of the legs. *Med. J. Aust.* **1983**, *2*, 279–283 10.5694/J.1326-5377.1983.TB122464.X.
41. Roy, R.; Haase, T.; Ma, N.; Bader, A.; Becker, M.; Seifert, M.; Choi, Y. H.; Falk, V.; Stamm, C. Decellularized amniotic membrane attenuates postinfarct left ventricular remodeling. *J. Surg. Res.* **2016**, *200*, 409–419 10.1016/j.jss.2015.08.022.
42. Roy, R.; Kukucka, M.; Messroghli, D.; Kunkel, D.; Brodarac, A.; Klose, K.; Geißler, S.; Becher, P. M.; Kang, S. K.; Choi, Y.-H.; Stamm, C. Epithelial-to-Mesenchymal Transition Enhances the Cardioprotective Capacity of Human Amniotic Epithelial Cells. *Cell Transplant.* **2015**, *24*, 985–1002 10.3727/096368913X675151.
43. Oberwallner, B.; Anic, B. A.; Šaric, W.; Kneef, K.; Choi, Y.-H.; Oberwallner, B.; Brodarac, A.; Anicá, P.; Šaric, T.; Wassilew, K.; Neef, K.; Choi, Y.-H.; Stamm, C. Human cardiac extracellular matrix supports myocardial lineage commitment of pluripotent stem cells. *Eur J Cardiothorac Surg* **2015**, *47*, 416–25 10.1093/ejcts/ezu163.
44. Frantz, C.; Stewart, K. M.; Weaver, V. M. The extracellular matrix at a glance. *J Cell Sci* **2010**, *123*, 4195–4200 10.1242/jcs.023820.
45. Burridge, K.; Turner, C. E.; Romer, L. H. Tyrosine phosphorylation of paxillin and pp125FAK accompanies cell adhesion to extracellular matrix: a role in cytoskeletal assembly. *J Cell Biol* **1992**, *119*, 893–903.
46. Peng, X.; Wu, X.; Druso, J. E.; Wei, H.; Park, A. Y.-J.; Kraus, M. S.; Alcaraz, A.; Chen, J.; Chien, S.; Cerione, R. A.; Guan, J.-L. Cardiac developmental defects and eccentric right ventricular hypertrophy in cardiomyocyte focal adhesion kinase (FAK) conditional knockout mice. *Proc. Natl. Acad. Sci. U. S. A.* **2008**, *105*, 6638–43 10.1073/pnas.0802319105.
47. Fujio, Y.; Nguyen, T.; Wencker, D.; Kitsis, R. N.; Walsh, K. Akt Promotes Survival of Cardiomyocytes In Vitro and Protects Against Ischemia-Reperfusion Injury in Mouse Heart. *Circulation* **2000**, *101*, 660–667.
48. Freytes, D. O.; Martin, J.; Velankar, S. S.; Lee, A. S.; Badylak, S. F. Preparation and rheological characterization of a gel form of the porcine urinary bladder matrix. *Biomaterials* **2008**, *29*, 1630–1637 10.1016/j.biomaterials.2007.12.014.
49. Robert A. Pouliot Ben Wong Rebecca L. Heise PhD., N. S. M. Extracellular Matrix Hydrogels from Decellularized Lung Tissue. **2015**.
50. DeQuach, J. A.; Mezzano, V.; Miglani, A.; Lange, S.; Keller, G. M.; Sheikh, F.; Christman, K. L. Simple and high yielding method for preparing tissue specific extracellular matrix coatings for cell culture. *PLoS One* **2010**, *5*, e13039 10.1371/journal.pone.0013039.
51. Singelyn, J. M.; DeQuach, J. A.; Seif-Naraghi, S. B.; Littlefield, R. B.; Schup-Magoffin, P. J.; Christman, K. L. Naturally derived myocardial matrix as an injectable scaffold for cardiac tissue engineering. *Biomaterials* **2009**, *30*, 5409–5416 10.1016/j.biomaterials.2009.06.045.
52. Singelyn, J. M.; Sundaramurthy, P.; Johnson, T. D.; Schup-Magoffin, P. J.; Hu, D. P.; Faulk, D. M.; Wang, J.; Mayle, K. M.; Bartels, K.; Salvatore, M.; Kinsey, A. M.; DeMaria, A. N.; Dib, N.; Christman, K. L. Catheter-Deliverable Hydrogel Derived From Decellularized Ventricular Extracellular Matrix Increases Endogenous Cardiomyocytes and Preserves Cardiac Function Post-Myocardial Infarction. *J. Am. Coll. Cardiol.* **2012**, *59*, 751–763 10.1016/j.jacc.2011.10.888.
53. Gaebel, R.; Ma, N.; Liu, J.; Guan, J.; Koch, L.; Klopsch, C.; Gruene, M.; Toelk, A.; Wang, W.; Mark, P.; Wang, F.; Chichkov, B.; Li, W.; Steinhoff, G. Patterning human stem cells and endothelial cells with laser printing for cardiac regeneration. *Biomaterials* **2011**, *32*, 9218–9230 10.1016/J.BIOMATERIALS.2011.08.071.
54. Zhang, J.; Klos, M.; Wilson, G. F.; Herman, A. M.; Lian, X.; Raval, K. K.; Barron, M. R.; Hou, L.; Soerens, A. G.; Yu, J.; Palecek, S. P.; Lyons, G. E.; Thomson, J. A.; Herron, T. J.; Jalife, J.; Kamp, T. J. Extracellular matrix promotes highly efficient cardiac differentiation of human pluripotent stem cells: The matrix sandwich method. *Circ. Res.* **2012**, *111*, 1125–1136 10.1161/CIRCRESAHA.112.273144.
55. Franz, S.; Rammelt, S.; Scharnweber, D.; Simon, J. C. Immune responses to implants - a review of the implications for the design of immunomodulatory biomaterials. *Biomaterials* **2011**, *32*, 6692–6709 10.1016/j.biomaterials.2011.05.078.
56. Johnson, T. D.; Dequach, J. A.; Gaetani, R.; Ungerleider, J.; Elhag, D.; Nigam, V.; Behfar, A.; Christman, K. L. Human versus porcine tissue sourcing for an injectable myocardial matrix hydrogel. *Biomater Sci* **2014**, *2014*, 60283D 10.1039/C3BM60283D.
57. Becker, M.; Maring, J.; Schneider, M.; Herrera Martin, A.; Seifert, M.; Klein, O.; Braun, T.; Falk, V.; Stamm, C. Towards a Novel Patch Material for Cardiac Applications: Tissue-Specific Extracellular Matrix Introduces Essential Key Features to Decellularized Amniotic Membrane. *Int. J. Mol. Sci.* **2018**, *19*, 1032 10.3390/ijms19041032.
58. Becker, M.; Maring, J. A.; Oberwallner, B.; Kappler, B.; Klein, O.; Falk, V.; Stamm, C. Processing of Human Cardiac Tissue Toward Extracellular Matrix Self-assembling Hydrogel for In Vitro and In Vivo Applications. *J. Vis. Exp.* **2017** 10.3791/56419, DOI 10.3791/56419.
59. Kappler, B.; Anic, P.; Becker, M.; Bader, A.; Klose, K.; Klein, O.; Oberwallner, B.; Choi, Y. H.; Falk, V.; Stamm, C. The cytoprotective capacity of processed human cardiac extracellular matrix. *J. Mater. Sci. Mater. Med.* **2016** 10.1007/s10856-016-5730-5, DOI 10.1007/s10856-016-5730-5.
60. Chang, C. W.; Petrie, T.; Clark, A.; Gaitan-Leon, D. Mesenchymal Stem Cell Seeding of Porcine Small Intestinal Submucosal Extracellular Matrix for Cardiovascular Applications. *PLoS One* **2016**, *11*, e0153412 10.1371/journal.pone.0153412.
61. Sadtler, K.; Estrellas, K.; Allen, B. W.; Wolf, M. T.; Fan, H.; Tam, A. J.; Patel, C. H.; Luber, B. S.; Wang, H.; Wagner, K. R.; Powell, J. D.; Housseau, F.; Pardoll, D. M.; Elisseeff, J. H. Developing a pro-regenerative biomaterial scaffold microenvironment requires T helper 2 cells. *Science* **2016**, *352*, 366–70 10.1126/science.aad9272.
62. Brown, B. N.; Ratner, B. D.; Goodman, S. B.; Amar, S.; Badylak, S. F. Macrophage polarization: an opportunity for improved outcomes in biomaterials and regenerative medicine. *Biomaterials* **2012**, *33*, 3792–802 10.1016/j.biomaterials.2012.02.034.
63. Ma, Y.; Halade, G. V; Lindsey, M. L. Extracellular matrix and fibroblast communication following myocardial infarction. *J Cardiovasc Transl Res* **2012**, *5*, 848–857 10.1007/s12265-012-9398-z.
64. Hansen, N. U.; Genovese, F.; Leeming, D. J.; Karsdal, M. A. The importance of extracellular matrix for cell function and in vivo likeness. *Exp Mol Pathol* **2015**, *98*, 286–294 10.1016/j.yexmp.2015.01.006.
65. Chen, W. C. W.; Wang, Z.; Missinato, M. A.; Park, D. W.; Long, D. W.; Liu, H.-J.; Zeng, X.; Yates, N. A.; Kim, K.; Wang, Y. Decellularized zebrafish cardiac extracellular matrix induces mammalian heart regeneration. *Sci. Adv.* **2016**, *2*, e1600844–e1600844

10.1126/sciadv.1600844.
66. Fong, A. H.; Romero-López, M.; Heylman, C. M.; Keating, M.; Tran, D.; Sobrino, A.; Tran, A. Q.; Pham, H. H.; Fimbres, C.; Gershon, P. D.; Botvinick, E. L.; George, S. C.; Hughes, C. C. W. Three-Dimensional Adult Cardiac Extracellular Matrix Promotes Maturation of Human Induced Pluripotent Stem Cell-Derived Cardiomyocytes. *Tissue Eng. Part A* **2016**, *22*, 1016–1025 10.1089/ten.tea.2016.0027.
67. Wang, Q.; Yang, H.; Bai, A.; Jiang, W.; Li, X.; Wang, X.; Mao, Y.; Lu, C.; Qian, R.; Guo, F.; Ding, T.; Chen, H.; Chen, S.; Zhang, J.; Liu, C.; Sun, N. Functional engineered human cardiac patches prepared from nature's platform improve heart function after acute myocardial infarction. *Biomaterials* **2016**, *105*, 52–65 10.1016/j.biomaterials.2016.07.035.
68. Sarig, U.; Sarig, H.; De-Berardinis, E.; Chaw, S.-Y.; Nguyen, E. B. V.; Ramanujam, V. S.; Thang, V. D.; Al-Haddawi, M.; Liao, S.; Seliktar, D.; Kofidis, T.; Boey, F. Y. C.; Venkatraman, S. S.; Machluf, M. Natural myocardial ECM patch drives cardiac progenitor based restoration even after scarring. *Acta Biomater.* **2016**, *44*, 209–220 10.1016/j.actbio.2016.08.031.
69. Slivka, P. F.; Dearth, C. L.; Keane, T. J.; Meng, F. W.; Medberry, C. J.; Riggio, R. T.; Reing, J. E.; Badylak, S. F.; Takeyama, H.; Feng, L.; Liang, Y. M.; Han, H.; DeQuach, J. A.; Preul, M.; Kinsey, A. M.; DeMaria, A. N.; Dib, N.; Christman, K. L.; Scherle, P. A.; Trzaskos, J. M.; Magolda, R. L.; Trainor, G. L.; Wexler, R. R.; Hobbs, F. W.; Olson, R. E. Fractionation of an ECM hydrogel into structural and soluble components reveals distinctive roles in regulating macrophage behavior. *Biomater. Sci.* **2014**, *2*, 1521–1534 10.1039/C4BM00189C.
70. Wolf, M. T.; Dearth, C. L.; Ranallo, C. A.; LoPresti, S. T.; Carey, L. E.; Daly, K. A.; Brown, B. N.; Badylak, S. F. Macrophage polarization in response to ECM coated polypropylene mesh. *Biomaterials* **2014**, *35*, 6838–6849 10.1016/j.biomaterials.2014.04.115.
71. Dziki, J. L.; Wang, D. S.; Pineda, C.; Sicari, B. M.; Rausch, T.; Badylak, S. F. Solubilized extracellular matrix bioscaffolds derived from diverse source tissues differentially influence macrophage phenotype. *J. Biomed. Mater. Res. - Part A* **2017**, *105*, 138–147 10.1002/jbm.a.35894.
72. Williams, C.; Quinn, K. P.; Georgakoudi, I.; Black, L. D. Young developmental age cardiac extracellular matrix promotes the expansion of neonatal cardiomyocytes in vitro. *Acta Biomater.* **2014**, *10*, 194–204 10.1016/j.actbio.2013.08.037.
73. Faulk, D. M.; Londono, R.; Wolf, M. T.; Ranallo, C. A.; Carruthers, C. A.; Wildemann, J. D.; Dearth, C. L.; Badylak, S. F. ECM hydrogel coating mitigates the chronic inflammatory response to polypropylene mesh. *Biomaterials* **2014**, *35*, 8585–8595 10.1016/j.biomaterials.2014.06.057.
74. Godier-Furnémont, A. F. G.; Martens, T. P.; Koeckert, M. S.; Wan, L.; Parks, J.; Arai, K.; Zhang, G.; Hudson, B.; Homma, S.; Vunjak-Novakovic, G. Composite scaffold provides a cell delivery platform for cardiovascular repair. *Proc. Natl. Acad. Sci. U. S. A.* **2011**, *108*, 7974–9 10.1073/pnas.1104619108.
75. Oberwallner, B.; Brodarac, A.; Choi, Y.-H.; Saric, T.; Anić, P.; Morawietz, L.; Stamm, C. Preparation of cardiac extracellular matrix scaffolds by decellularization of human myocardium. *J. Biomed. Mater. Res. Part A* **2014**, *102*, 3263–3272 10.1002/jbm.a.35000.
76. Williams, C.; Sullivan, K.; Black, L. D. Partially Digested Adult Cardiac Extracellular Matrix Promotes Cardiomyocyte Proliferation In Vitro. *Adv. Healthc. Mater.* **2015**, *4*, 1545–1554 10.1002/adhm.201500035.
77. Bejleri, D.; Streeter, B. W.; Nachlas, A. L. Y.; Brown, M. E.; Gaetani, R.; Christman, K. L.; Davis, M. E. A Bioprinted Cardiac Patch Composed of Cardiac-Specific Extracellular Matrix and Progenitor Cells for Heart Repair. *Adv. Healthc. Mater.* **2018**, *7*, 1800672 10.1002/adhm.201800672.
78. Jang, J.; Park, H.-J.; Kim, S.-W.; Kim, H.; Park, J. Y.; Na, S. J.; Kim, H. J.; Park, M. N.; Choi, S. H.; Park, S. H.; Kim, S. W.; Kwon, S.-M.; Kim, P.-J.; Cho, D.-W. 3D printed complex tissue construct using stem cell-laden decellularized extracellular matrix bioinks for cardiac repair. *Biomaterials* **2017**, *112*, 264–274 10.1016/J.BIOMATERIALS.2016.10.026.
79. "BRENDA - Information on EC 3.4.23.1 - pepsin A," can be found under https://www.brenda-enzymes.org/enzyme.php?ecno=3.4.23.1#pH OPTIMUM, **n.d.**
80. Chen, L.; Wang, Y.; Pan, Y.; Zhang, L.; Shen, C.; Qin, G.; Ashraf, M.; Weintraub, N.; Ma, G.; Tang, Y. Cardiac progenitor-derived exosomes protect ischemic myocardium from acute ischemia/reperfusion injury. *Biochem. Biophys. Res. Commun.* **2013** 10.1016/j.bbrc.2013.01.015, DOI 10.1016/j.bbrc.2013.01.015.
81. Maring, J. A.; Lodder, K.; Mol, E.; Verhage, V.; Wiesmeijer, K. C.; Dingenouts, C. K. E.; Moerkamp, A. T.; Deddens, J. C.; Vader, P.; Smits, A. M.; Sluijter, J. P. G.; Goumans, M. J. Cardiac Progenitor Cell–Derived Extracellular Vesicles Reduce Infarct Size and Associate with Increased Cardiovascular Cell Proliferation. *J. Cardiovasc. Transl. Res.* **2018** 10.1007/s12265-018-9842-9, DOI 10.1007/s12265-018-9842-9.
82. Ibrahim, A. G. E.; Cheng, K.; Marbán, E. Exosomes as critical agents of cardiac regeneration triggered by cell therapy. *Stem Cell Reports* **2014** 10.1016/j.stemcr.2014.04.006, DOI 10.1016/j.stemcr.2014.04.006.
83. Halkein, J.; Tabruyn, S. P.; Ricke-Hoch, M.; Haghikia, A.; Nguyen, N. Q. N.; Scherr, M.; Castermans, K.; Malvaux, L.; Lambert, V.; Thiry, M.; Sliwa, K.; Noel, A.; Martial, J. A.; Hilfiker-Kleiner, D.; Struman, I. MicroRNA-146a is a therapeutic target and biomarker for peripartum cardiomyopathy. *J. Clin. Invest.* **2013** 10.1172/JCI64365, DOI 10.1172/JCI64365.
84. Yamaguchi, T.; Izumi, Y.; Nakamura, Y.; Yamazaki, T.; Shiota, M.; Sano, S.; Tanaka, M.; Osada-Oka, M.; Shimada, K.; Miura, K.; Yoshiyama, M.; Iwao, H. Repeated remote ischemic conditioning attenuates left ventricular remodeling via exosome-mediated intercellular communication on chronic heart failure after myocardial infarction. *Int. J. Cardiol.* **2015** 10.1016/j.ijcard.2014.10.144, DOI 10.1016/j.ijcard.2014.10.144.
85. Huleihel, L.; Hussey, G. S.; Naranjo, J. D.; Zhang, L.; Dziki, J. L.; Turner, N. J.; Stolz, D. B.; Badylak, S. F. Matrix-bound nanovesicles within ECM bioscaffolds. *Sci. Adv.* **2016**, *2*, e1600502–e1600502 10.1126/sciadv.1600502.
86. An, M.; Kwon, K.; Park, J.; Ryu, D. R.; Shin, J. A.; Lee Kang, J.; Choi, J. H.; Park, E. M.; Lee, K. E.; Woo, M.; Kim, M. Extracellular matrix-derived extracellular vesicles promote cardiomyocyte growth and electrical activity in engineered cardiac atria. *Biomaterials* **2017**, *146*, 49–59 10.1016/j.biomaterials.2017.09.001.
87. Rowland, R. N.; Woodley, J. F. The stability of liposomes in vitro to pH, bile salts and pancreatic lipase. *Biochim. Biophys. Acta - Lipids Lipid Metab.* **1980**, *620*, 400–409 10.1016/0005-2760(80)90131-9.
88. Khalpey, Z.; Marsh, K. M.; Ferng, A.; Riaz, I. Bin; Friedman, M.; Indik, J.; Avery, R.; Jokerst, C.; Oliva, I. First in man: amniotic patch reduces postoperative inflammation. *Am. J. Med.* **2015**, *128*, e5-6 10.1016/j.amjmed.2014.08.028.
89. Cargnoni, A.; Di Marcello, M.; Campagnol, M.; Nassuato, C.; Albertini, A.; Parolini, O. Amniotic Membrane Patching Promotes Ischemic Rat Heart Repair. *Cell Transplant.* **2009**, *18*, 1147–1159 10.3727/096368909X12483162196764.
90. Sant'anna, L. B.; Cargnoni, A.; Ressel, L.; Vanosi, G.; Parolini, O. Amniotic Membrane Application Reduces Liver Fibrosis in a Bile Duct Ligation Rat Model. *Cell Transplant.* **2011**, *20*, 441–453 10.3727/096368910X522252.
91. Tosi, G. M.; Massaro-Giordano, M.; Caporossi, A.; Toti, P. Amniotic membrane transplantation in ocular surface disorders. *J. Cell. Physiol.* **2005**, *202*, 849–851 10.1002/jcp.20181.
92. Tang, J.; Vandergriff, A.; Wang, Z.; Hensley, M. T.; Cores, J.; Allen, T. A.; Dinh, P.-U.; Zhang, J.; Caranasos, T. G.; Cheng, K. A Regenerative Cardiac Patch Formed by Spray Painting of Biomaterials onto the Heart. *TISSUE Eng. Part C* **2017**, *23* 10.1089/ten.tec.2016.0492, DOI 10.1089/ten.tec.2016.0492.
93. Brown, J. H.; Das, P.; DiVito, M. D.; Ivancic, D.; Tan, L. P.; Wertheim, J. A. Nanofibrous PLGA electrospun scaffolds modified with type I collagen influence hepatocyte function and support viability in vitro. *Acta Biomater.* **2018**, *73*, 217–227

10.1016/J.ACTBIO.2018.02.009.
94. Wolf, M. T.; Carruthers, C. A.; Dearth, C. L.; Crapo, P. M.; Huber, A.; Burnsed, O. A.; Londono, R.; Johnson, S. A.; Daly, K. A.; Stahl, E. C.; Freund, J. M.; Medberry, C. J.; Carey, L. E.; Nieponice, A.; Amoroso, N. J.; Badylak, S. F. Polypropylene surgical mesh coated with extracellular matrix mitigates the host foreign body response. *J. Biomed. Mater. Res. Part A* **2014**, *102*, 234–246 10.1002/jbm.a.34671.
95. Lee, J.; Tae, G.; Kim, Y. H.; Park, I. S.; Kim, S.-H.; Kim, S. H. The effect of gelatin incorporation into electrospun poly(l-lactide-co-ε-caprolactone) fibers on mechanical properties and cytocompatibility. *Biomaterials* **2008**, *29*, 1872–1879 10.1016/J.BIOMATERIALS.2007.12.029.
96. Gu, X.; Matsumura, Y.; Tang, Y.; Roy, S.; Hoff, R.; Wang, B.; Wagner, W. R. Sustained viral gene delivery from a micro-fibrous, elastomeric cardiac patch to the ischemic rat heart. *Biomaterials* **2017**, *133*, 132–143 10.1016/j.biomaterials.2017.04.015.
97. Du, J.; Zu, Y.; Li, J.; Du, S.; Xu, Y.; Zhang, L.; Jiang, L.; Wang, Z.; Chien, S.; Yang, C. Extracellular matrix stiffness dictates Wnt expression through integrin pathway. *Sci Rep* **2016**, *6*, 20395 10.1038/srep20395.
98. Ribeiro, A. J.; Ang, Y. S.; Fu, J. D.; Rivas, R. N.; Mohamed, T. M.; Higgs, G. C.; Srivastava, D.; Pruitt, B. L. Contractility of single cardiomyocytes differentiated from pluripotent stem cells depends on physiological shape and substrate stiffness. *Proc Natl Acad Sci U S A* **2015** 10.1073/pnas.1508073112, DOI 10.1073/pnas.1508073112.
99. Mit-uppatham, C.; Nithitanakul, M.; Supaphol, P. Ultrafine Electrospun Polyamide-6 Fibers: Effect of Solution Conditions on Morphology and Average Fiber Diameter. *Macromol. Chem. Phys.* **2004**, *205*, 2327–2338 10.1002/macp.200400225.
100. Claycomb, W. C.; Lanson, N. A.; Stallworth, B. S.; Egeland, D. B.; Delcarpio, J. B.; Bahinski, A.; Izzo, N. J. HL-1 cells: a cardiac muscle cell line that contracts and retains phenotypic characteristics of the adult cardiomyocyte. *Proc. Natl. Acad. Sci. U. S. A.* **1998**, *95*, 2979–84 10.1073/PNAS.95.6.2979.
101. Han, C.; Nie, Y.; Lian, H.; Liu, R.; He, F.; Huang, H.; Hu, S. Acute inflammation stimulates a regenerative response in the neonatal mouse heart. *Cell Res* **2015** 10.1038/cr.2015.110, DOI 10.1038/cr.2015.110.
102. Grotenhuis, N.; vd Toom, H. F. E.; Kops, N.; Bayon, Y.; Deerenberg, E. B.; Mulder, I. M.; van Osch, G. J. V. M.; Lange, J. F.; Bastiaansen-Jenniskens, Y. M. *In vitro* model to study the biomaterial-dependent reaction of macrophages in an inflammatory environment. *Br. J. Surg.* **2014**, *101*, 983–992 10.1002/bjs.9523.
103. Ariganello, M. B.; Simionescu, D. T.; Labow, R. S.; Michael Lee, J. Macrophage differentiation and polarization on a decellularized pericardial biomaterial. *Biomaterials* **2011**, *32*, 439–449 10.1016/J.BIOMATERIALS.2010.09.004.
104. van Amerongen, M. J.; Harmsen, M. C.; van Rooijen, N.; Petersen, A. H.; van Luyn, M. J. A. Macrophage Depletion Impairs Wound Healing and Increases Left Ventricular Remodeling after Myocardial Injury in Mice. *Am. J. Pathol.* **2007**, *170*, 818–829 10.2353/AJPATH.2007.060547.
105. Vitkov, L.; Krautgartner, W.-D.; Obermayer, A.; Stoiber, W.; Hannig, M.; Klappacher, M.; Hartl, D. The Initial Inflammatory Response to Bioactive Implants Is Characterized by NETosis. *PLoS One* **2015**, *10*, e0121359 10.1371/journal.pone.0121359.
106. Taraballi, F.; Sushnitha, M.; Tsao, C.; Bauza, G.; Liverani, C.; Shi, A.; Tasciotti, E. Biomimetic Tissue Engineering: Tuning the Immune and Inflammatory Response to Implantable Biomaterials. *Adv. Healthc. Mater.* **2018**, *7*, 1800490 10.1002/adhm.201800490.
107. Opasawatchai, A.; Amornsupawat, P.; Jiravejchakul, N.; Chan-In, W.; Spoerk, N. J.; Manopwisedjaroen, K.; Singhasivanon, P.; Yingtaweesak, T.; Suraamornkul, S.; Mongkolsapaya, J.; Sakuntabhai, A.; Matangkasombut, P.; Loison, F. Neutrophil Activation and Early Features of NET Formation Are Associated With Dengue Virus Infection in Human. *Front. Immunol.* **2018**, *9*, 3007 10.3389/fimmu.2018.03007.
108. Hertwig, L.; Pache, F.; Romero-Suarez, S.; Stürner, K. H.; Borisow, N.; Behrens, J.; Bellmann-Strobl, J.; Seeger, B.; Asselborn, N.; Ruprecht, K.; Millward, J. M.; Infante-Duarte, C.; Paul, F. Distinct functionality of neutrophils in multiple sclerosis and neuromyelitis optica. *Mult. Scler. J.* **2016**, *22*, 160–173 10.1177/1352458515586084.
109. Dong, Y.; Lagarde, J.; Xicota, L.; Corne, H.; Chantran, Y.; Chaigneau, T.; Crestani, B.; Bottlaender, M.; Potier, M.-C.; Aucouturier, P.; Dorothée, G.; Sarazin, M.; Elbim, C. Neutrophil hyperactivation correlates with Alzheimer's disease progression. *Ann. Neurol.* **2018**, *83*, 387–405 10.1002/ana.25159.
110. Rajeeve, K.; Das, S.; Prusty, B. K.; Rudel, T. Chlamydia trachomatis paralyses neutrophils to evade the host innate immune response. *Nat. Microbiol.* **2018**, *3*, 824–835 10.1038/s41564-018-0182-y.
111. Wellappuli, N. C.; Fine, N.; Lawrence, H. P.; Goldberg, M.; Tenenbaum, H. C.; Glogauer, M. Oral and Blood Neutrophil Activation States during Experimental Gingivitis. *JDR Clin. Transl. Res.* **2018**, *3*, 65–75 10.1177/2380084417742120.
112. Ma, Y.; Yabluchanskiy, A.; Iyer, R. P.; Cannon, P. L.; Flynn, E. R.; Jung, M.; Henry, J.; Cates, C. A.; Deleon-Pennell, K. Y.; Lindsey, M. L. Temporal neutrophil polarization following myocardial infarction. *Cardiovasc. Res.* **2016**, *110*, 51–61 10.1093/cvr/cvw024.
113. Marchi, L. F.; Sesti-Costa, R.; Ignacchiti, M. D. C.; Chedraoui-Silva, S.; Mantovani, B. In vitro activation of mouse neutrophils by recombinant human interferon-gamma: Increased phagocytosis and release of reactive oxygen species and pro-inflammatory cytokines. *Int. Immunopharmacol.* **2014**, *18*, 228–235 10.1016/j.intimp.2013.12.010.
114. Musso, T.; Calosso, L.; Zucca, M.; Millesimo, M.; Puliti, M.; Bulfone-Paus, S.; Merlino, C.; Savoia, D.; Cavallo, R.; Ponzi, A. N.; Badolato, R. Interleukin-15 activates proinflammatory and antimicrobial functions in polymorphonuclear cells. *Infect. Immun.* **1998**, *66*, 2640–2647.
115. Colotta, F.; Re, F.; Polentarutti, N.; Sozzani, S.; Mantovani, A. Modulation of granulocyte survival and programmed cell death by cytokines and bacterial products. *Blood* **1992**, *80*, 2012–20 1382715.
116. Shalaby, M. R.; Aggarwal, B. B.; Rinderknecht, E.; Svedersky, L. P.; Finkle, B. S.; Palladino, M. a Activation of human polymorphonuclear neutrophil functions by interferon-gamma and tumor necrosis factors. *J. Immunol.* **1985**, *135*, 2069–2073.
117. Hertwig, L.; Pache, F.; Romero-Suarez, S.; Stürner, K. H.; Borisow, N.; Behrens, J.; Bellmann-Strobl, J.; Seeger, B.; Asselborn, N.; Ruprecht, K.; Millward, J. M.; Infante-Duarte, C.; Paul, F. Distinct functionality of neutrophils in multiple sclerosis and neuromyelitis optica. *Mult. Scler.* **2015**, *22*, 1–14 10.1177/1352458515586084.
118. Kikuchi, K.; Holdway, J. E.; Werdich, A. A.; Anderson, R. M.; Fang, Y.; Egnaczyk, G. F.; Evans, T.; Macrae, C. A.; Stainier, D. Y.; Poss, K. D. Primary contribution to zebrafish heart regeneration by gata4(+) cardiomyocytes. *Nature* **2010**, *464*, 601–605 10.1038/nature08804.

[auch Bestandteil der Dissertation]

EIDESSTATTLICHE VERSICHERUNG

„Ich, Matthias Becker, versichere an Eides statt durch meine eigenhändige Unterschrift, dass ich die vorgelegte Dissertation mit dem Thema: Development of a bioactive epicardial composite patch for support of myocardial regeneration selbstständig und ohne nicht offengelegte Hilfe Dritter verfasst und keine anderen als die angegebenen Quellen und Hilfsmittel genutzt habe.
Alle Stellen, die wörtlich oder dem Sinne nach auf Publikationen oder Vorträgen anderer Autoren beruhen, sind als solche in korrekter Zitierung kenntlich gemacht. Die Abschnitte zu Methodik (insbesondere praktische Arbeiten, Laborbestimmungen, statistische Aufarbeitung) und Resultaten (insbesondere Abbildungen, Graphiken und Tabellen) werden von mir verantwortet.

Meine Anteile an etwaigen Publikationen zu dieser Dissertation entsprechen denen, die in der untenstehenden gemeinsamen Erklärung mit dem/der Betreuer/in, angegeben sind. Für sämtliche im Rahmen der Dissertation entstandenen Publikationen wurden die Richtlinien des ICMJE (International Committee of Medical Journal Editors; www.icmje.og) zur Autorenschaft eingehalten. Ich erkläre ferner, dass mir die Satzung der Charité – Universitätsmedizin Berlin zur Sicherung Guter Wissenschaftlicher Praxis bekannt ist und ich mich zur Einhaltung dieser Satzung verpflichte.

Die Bedeutung dieser eidesstattlichen Versicherung und die strafrechtlichen Folgen einer unwahren eidesstattlichen Versicherung (§156,161 des Strafgesetzbuches) sind mir bekannt und bewusst.“

Datum _____ Unterschrift

Anteilserklärung an den erfolgten Publikationen

[Die Anteile an den jeweiligen Publikationen sind so deutlich und detailliert zu erklären, dass es der Promotionskommission und den wissenschaftlichen Gutachtern ohne Probleme möglich ist zu erkennen, was Sie selbst dazu beigetragen haben. Wünschenswert wäre ein konkreter Bezug zur Publikation wie z. B.: „aus meiner statistischen Auswertung sind die Tabellen 1, 4, 47 und 60 entstanden.“]

Matthias Becker hatte folgenden Anteil an den folgenden Publikationen:

Publikation 1: Benjamin Kappler, Petra Anic, **Matthias Becker**, Andreas Bader, Kristin Klose, Oliver Klein, Barbara Oberwallner, Yeong-Hoon Choi, Volkmar Falk, Christof Stamm; *The cytoprotective capacity of processed human cardiac extracellular matrix*; Journal of Materials Science: Materials in Medicine; 2016

In meiner Verantwortung lag die weitere Prozessierung der ECM Partikel und Entwicklung des ECM Hydrogels. Ich korrigierte das bestehende Protokoll und konnte eine Prozessierung entwickeln, die zu einem ECM Hydrogel führte, das sowohl gelieren konnte, als auch, im Gegensatz zur Ausgangsituation, zytoprotektiv wirkte. Literaturforschung, Design und Durchführung der Experimente, Datenerhebung, statistische Auswertung sowie Bildaufnahmen sind selbstständig und eigenverantwortlich von mir durchgeführt. Durch meine Beiträge sind die Figuren 2 und 6 entstanden.

Publikation 2: **Matthias Becker**, Janita A. Maring, Barbara Oberwallner, Benjamin Kappler, Oliver Klein, Volkmar Falk, Christof Stamm; *Processing of Human Cardiac Tissue Toward Extracellular Matrix Self-assembling Hydrogel for In Vitro and In Vivo Applications*; Journal of Visualized Experiments, 2017

Als Erst-Author ist diese Arbeit nahezu vollständig durch mich veröffentlicht worden. Ich verantwortet ergänzendes Design und Durchführung der Experimente, Skizzieren des Manuskripts und damit verbundene Klärung des Copyrights verwendeter Figuren, Erstellen des Manuskripts mit Ergänzungen der Co-Authoren, Interaktion mit dem Journal und Editoren sowie Durchführung aller Schritte und Korrekturen der Revision. Durch meine Beiträge sind die Figuren 1,3,4,5 und Tabelle 1 entstanden bzw. verwendet worden. Weiterhin habe ich die finale Videodemonstration vorbereitet, geplant, koordiniert und durchgeführt.

Publikation 3: **Matthias Becker**, Janita A. Maring, Maria Schneider, Aarón X. Herrera Martin, Martina Seifert, Oliver Klein, Thorsten Braun, Volkmar Falk, Christof Stamm; *Towards a Novel Patch Material for Cardiac Applications: Tissue-Specific Extracellular Matrix Introduces Essential Key Features to Decellularized Amniotic Membrane*; International Journal of Molecular Science; 2018

Als Erst-Author ist diese Arbeit nahezu vollständig durch mich veröffentlicht worden. Literaturforschung, Probenvorbereitung, Design und Durchführung der Experimente, Datenerhebung, statistische Auswertung sowie Bildaufnahmen sind selbstständig und eigenverantwortlich von mir durchgeführt. Alle Figuren sind durch meine Beiträge entstanden. Zudem lag es in meiner Verantwortung Skizzieren und Erstellen des Manuskripts mit Ergänzungen der Co-Authoren, Interaktion mit dem Journal und Editoren sowie Durchführung aller Schritte und Korrekturen der Revision durchzuführen.

_____

Unterschrift, Datum und Stempel des betreuenden Hochschullehrers/der betreuenden Hochschullehrerin

_____

Unterschrift des Doktoranden/der Doktorandin

PUBLIKATION 1

THE CYTOPROTECTIVE CAPACITY OF PROCESSED HUMAN CARDIAC EXTRACELLULAR MATRIX

Kappler, B., Anic, P., **Becker, M**., Bader, A., Klose, K., Klein, O., ... & Stamm, C. (2016). The cytoprotective capacity of processed human cardiac extracellular matrix. Journal of Materials Science: Materials in Medicine, 27(7), 120.

https://doi.org/10.1007/s10856-016-5730-5

PUBLIKATION 2

PROCESSING OF HUMAN CARDIAC TISSUE TOWARD EXTRACELLULAR MATRIX SELF-ASSEMBLING HYDROGEL FOR *IN VITRO* AND *IN VIVO* APPLICATIONS

Becker, M., Maring, J. A., Oberwallner, B., Kappler, B., Klein, O., Falk, V., & Stamm, C. (2017). Processing of human cardiac tissue toward extracellular matrix self-assembling hydrogel for in vitro and in vivo applications. JoVE (Journal of Visualized Experiments), (130), e56419.

https://doi.org/doi:10.3791/56419

PUBLIKATION 3

TOWARDS A NOVEL PATCH MATERIAL FOR CARDIAC APPLICATIONS: TISSUE-SPECIFIC EXTRACELLULAR MATRIX INTRODUCES ESSENTIAL KEY FEATURES TO DECELLULARIZED AMNIOTIC MEMBRANE

Becker, M., Maring, J. A., Schneider, M., Martin, H., Aarón, X., Seifert, M., ... & Stamm, C. (2018). Towards a novel patch material for cardiac applications: tissue-specific extracellular matrix introduces essential key features to decellularized amniotic membrane. International journal of molecular sciences, 19(4), 1032.

https://doi.org/10.3390/ijms19041032

International Journal of
Molecular Sciences

MDPI

Article

Towards a Novel Patch Material for Cardiac Applications: Tissue-Specific Extracellular Matrix Introduces Essential Key Features to Decellularized Amniotic Membrane

Matthias Becker [1,2], Janita A. Maring [1,2], Maria Schneider [1,2], Aarón X. Herrera Martin [1,3], Martina Seifert [1,2], Oliver Klein [1,2], Thorsten Braun [4], Volkmar Falk [2,5,6] and Christof Stamm [1,2,5,6,*]

1 Charité—Universitätsmedizin Berlin, Corporate Member of Freie Universität Berlin, Humboldt-Universität zu Berlin, and Berlin Institute of Health, 13353 Berlin, Germany; matthias.becker@charite.de (M.B.); josemaring@hotmail.com (J.A.M.); maria.schneider@charite.de (M.Sc.); aaron.herrera@charite.de (A.X.H.M.) martina.seifert@charite.de (M.Se.); oliver.klein@charite.de (O.K.)
2 Berlin-Brandenburg Center for Regenerative Therapies (BCRT), 13353 Berlin, Germany; falk@dhzb.de
3 Julius Wolff Institute for Biomechanics and Musculoskeletal Regeneration, 13353 Berlin, Germany
4 Department of Obstetrics and Gynecology, Charite Medical University, 13353 Berlin, Germany; thorsten.braun@charite.de
5 German Centre for Cardiovascular Research (DZHK), Partner Site Berlin, 13316 Berlin, Germany
6 Deutsches Herzzentrum Berlin (DHZB), Augustenburger Platz 1, 13353 Berlin, Germany
* Correspondence: stamm@dhzb.de; Tel.: +49-30-453-321-09

Received: 9 March 2018; Accepted: 27 March 2018; Published: 29 March 2018

Abstract: There is a growing need for scaffold material with tissue-specific bioactivity for use in regenerative medicine, tissue engineering, and for surgical repair of structural defects. We developed a novel composite biomaterial by processing human cardiac extracellular matrix (ECM) into a hydrogel and combining it with cell-free amniotic membrane via a dry-coating procedure. Cardiac biocompatibility and immunogenicity were tested in vitro using human cardiac fibroblasts, epicardial progenitor cells, murine HL-1 cells, and human immune cells derived from buffy coat. Processing of the ECM preserved important matrix proteins as demonstrated by mass spectrometry. ECM coating did not alter the mechanical characteristics of decellularized amniotic membrane but did cause a clear increase in adhesion capacity, cell proliferation and viability. Activated monocytes secreted less pro-inflammatory cytokines, and both macrophage polarization towards the pro-inflammatory M1 type and T cell proliferation were prevented. We conclude that the incorporation of human cardiac ECM hydrogel shifts and enhances the bioactivity of decellularized amniotic membrane, facilitating its use in future cardiac applications.

Keywords: extracellular matrix; hydrogel; cardioprotection; patch; epicardium; amnion; immunocompatibility

1. Introduction

Cardiovascular disease remains the leading cause of death in industrialized societies and is on the rise in developing countries [1]. For end-stage heart failure, there is currently no effective therapeutic alternative other than heart transplantation or mechanical assist device implantation, because the regenerative potential of the postnatal mammalian myocardium is insufficient to restore function to the damaged heart [2]. Intramyocardial or intravascular cell transplantation techniques were considered promising regenerative strategies but largely underperformed in clinical trials. For instance,

Hastings et al. [3] compared intramyocardial injections of different stem and progenitor cell products and demonstrated the limited performance in in vivo models and clinical applications. This lack of efficacy can be explained by the poor retention of injected cells in the infarcted tissue [4], and it has been published that the application of therapeutics via an epicardial patch system is more effective in creating a sustained effect [5].

As a translationally competent biologic human scaffold system, we have previously shown that decellularized human amniotic membrane alone reduces post-infarct remodeling processes if applied epicardially [6]. However, its pro-regenerative and immunomodulatory capacity may be further enhanced by modulating the protein composition and incorporating target tissue-specific bioactivity [7,8]. So far, the majority of compounds used for these types of studies (e.g., Gelatin, collagen) have been highly defined prior to their use and were investigated individually [9–11], and we hypothesized that the use of an organ-specific protein composition would benefit the integration of the patch and aid regenerative processes.

We have previously succeeded in isolating Extracellular Matrix (ECM) from human myocardium (hcECM) with a more preserved protein composition compared to protocols reported by other groups [12], for example, with regards to glycosaminoglycans (GAG) [13], and demonstrated its capacity to support cell viability and induce cardiac lineage differentiation of pluripotent stem cells [14]. Furthermore, we demonstrated that the additional processing to microparticles and subsequent reconstitution as a hydrogel does not affect the cytoprotective capacity of the hcECM [15].

Here, we designed a novel composite patch material, linking the essential biological characteristics of target organ ECM with a stable carrier material by combining hcECM hydrogel (hgECM) with the cell-free amniotic membrane and tested its cytoprotective and immunological properties.

2. Results

2.1. Processing into Hydrogel Preserves Protein Composition

Processing into a hydrogel via Pepsin digestion may have a significant impact on ECM protein composition, greatly depending on the individual digestion and processing procedure [16,17]. We therefore examined the final protein composition of the hgECM after processing using mass spectrometry (MS).

A total of 113 proteins were identified in hgECM, of which 51 belong to the Extracellular Region Part (Figure 1) according to the STRING network database (Table S1), indicating that processing of the myocardium by decellularization, pulverization and homogenization preserved the majority of typical ECM proteins. For instance, different subtypes of collagen types 1, 3, 4, 5 and 6 were detected, as well as dermatopontin, fibrillin 1 and fibronectin 1, which are responsible for cell adhesions and Transforming Growth Factor beta (TGF-β) regulation. Other proteins involved in cell adhesion and matrix interaction were found including thrombospondin 1—a cell-to-cell and cell-to-matrix mediator—and vitronectin—a cell-to-substrate adhesion molecule and inhibitor of the membrane-damaging effect of the terminal cytolytic complement pathway.

Furthermore, several intracellular proteins were found that are involved in cell cycle, ECM regulation, or signaling pathway modifications such as acetyl-CoA acyltransferase 2, actin, actinin, different ATP synthases, complement component 3, desmin, chitinase, and heat shock 27 kDa protein 1. Thus, processing not only preserved a large number of ECM proteins but also cellular proteins relevant for cytoprotective support.

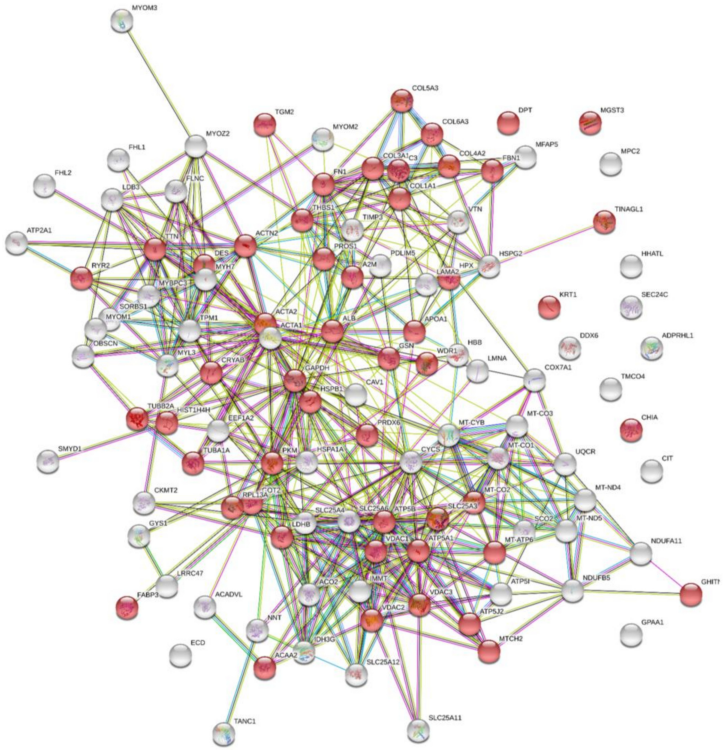

Figure 1. STRING analysis depicting hgECM proteins identified by MS. A total of 113 proteins were identified in the hgECM, of which 51 belong to the ECM region (red spheres). Lines indicate known protein interaction from curated databases (turquoise) and experimentally determined (pink), predicted interactions for gene neighborhood (green), gene fusion (red) and gene co-occurrence (blue). Other connections indicate text mining (yellow), co-expression (black) and protein homology (light blue). Detailed information on identified proteins is provided in Table S1.

2.2. DeAM Coating with hgECM Generates Novel Surfaces

Cell-free hcECM slices were processed into microparticles and homogenized into a hydrogel [13] to be used as a coating for decellularized amniotic membrane (DeAM). Scanning electron microscopy (SEM) was performed to visualize the shape of particles and the modified surface of hgECM coated DeAM (DeAM + E) in contrast to DeAM.

Pulverization of the hcECM resulted in microparticles with essentially uniform size and shape (Figure 2a,b). Further processing yielded a viscous hydrogel that was used to coat the DeAM carrier material. The structure of uncoated DeAM is shown in (Figure 2c,d). Coating of DeAM with hgECM (DeAM + E) did not change the global morphology as seen with low magnification (Figure 2e), but higher magnification revealed the hgECM generated an additional, unique nano-scale structure on top of the DeAM fibrillar architecture (Figure 2f) providing a modified structural surface.

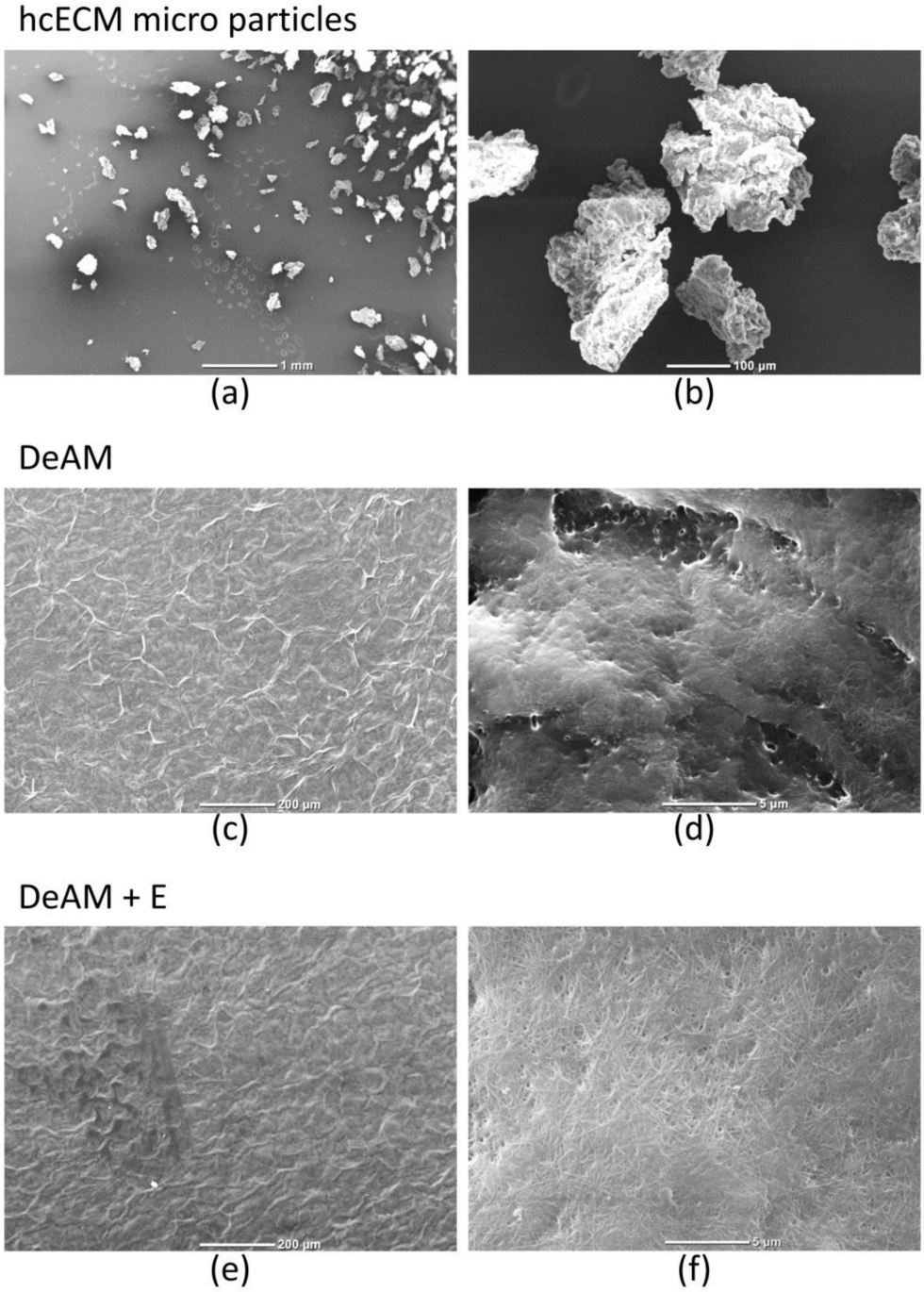

Figure 2. Scanning electron microscope visualization of hcECM microparticles as well as hgECM coated and uncoated DeAM. Structure analysis of patch components is shown as representative images. (**a**,**b**) SEM visualization of hcECM microparticles with a median particle feret diameter of 66 µm [15] ((**a**): magnification 20×; scale bar 1 mm; (**b**): magnification 170×; scale bar 100 µm); (**c**,**d**) Structure of DeAM ((**c**): magnification 100×; scale bar 200 µm; (**d**): magnification 5000×; scale bar 5 µm); (**e**,**f**) DeAM + E ((**e**): magnification 100×; scale bar 200 µm; (**f**): magnification 4500×; scale bar 5 µm).

2.3. Manipulation and Processing Do Not Affect the Mechanical Properties of Amniotic Membrane Scaffold Material

The elastic modulus (E-modulus) is an important factor of a material that determines how a material elastically deforms when pressure is applied, such as the pressure placed on the walls of the

heart by its movement. Once applied to the organ, the material must withstand the present stress, e.g., up to 0.5×10^6 Pa in the human heart [18]. Uniaxial pulling tests were performed for the different membranes to obtain the E-moduli as the relationship between the stress and strain of the linear region of the load curve. Maximum stress was obtained as the maximum load before sample rupture. However, rupture of the membranes occurred at the border near the clamps due to the stress concentrators produced by the patterned surface of the clamps, leading to micro-fractures in these areas that later propagate and lead to failure of the material. Therefore, the maximum stress values shown here represent a conservative case of the maximum stress that these membranes can withstand.

We examined the mechanical properties (E-modulus and maximum stress resistance) of the amniotic membrane (AM), the DeAM and the DeAM + E, to elucidate whether the processing of the AM affects the elastic behavior and stress resistance. Typical mechanical behavior of the membranes during a uniaxial pulling test was characterized by a toe region where the load was transferred to sample, a linear region where the E-modulus was obtained, and rupture once the maximum stress has been reached (Figure 3a). Graphical representation of the stress shows the limit of stress retention by the rapid decrease in Pa, while the slope indicates the E-modulus (Figure 3b). The mechanical properties for the analyzed membranes were not significantly different. The average E-moduli (Figure 3c) of AM, DeAM and DeAM + E were $8.8 \times 10^6 \pm 1.7 \times 10^6$ Pa, $8.2 \times 10^6 \pm 1.5 \times 10^6$ Pa and $9.9 \times 10^6 \pm 1.7 \times 10^6$ Pa, respectively. Maximum stress (Figure 3d) for the different membranes was $3.5 \times 10^6 \pm 1.7 \times 10^6$ Pa, $3.5 \times 10^6 \pm 1.6 \times 10^6$ Pa and $4.3 \times 10^6 \pm 1.5 \times 10^6$ Pa for AM, DeAM and DeAM + E respectively. These data confirm that the modified amniotic membrane has mechanical characteristics similar to those of native amniotic tissue. The maximum stress of the membranes is above the stress that the cardiac tissue is subjected to in vivo, indicating that membranes will withstand the physiological loads without failure. Therefore, they are suitable for implantation, surgical application and ultimately in clinical interventions.

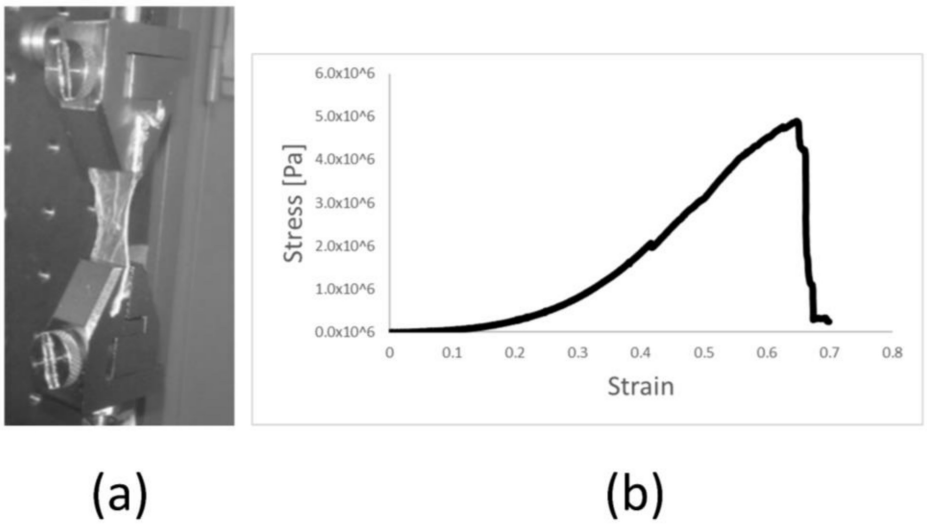

Figure 3. *Cont.*

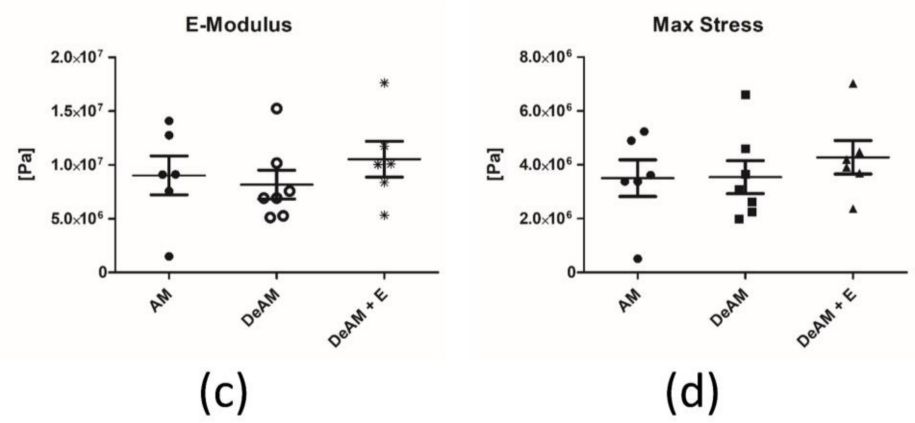

Figure 3. Determination of mechanical properties of the amniotic membrane (AM), the DeAM and the DeAM + E by the uniaxial pulling test. (**a**) Setup of horizontal pulling test, (**b**) Representative stress-strain curve, (**c**) single values E-modulus and (**d**) single values maximum stress resistance. $n \geq 6$.

2.4. hgECM Coating of DeAM Improves Cell Adhesion and Increases Viability

To examine the influence of hgECM coating on the biological properties of DeAM, we focused on selected cell types that are relevant for cardiac regeneration processes, namely, human cardiac fibroblasts (hCF), human epicardial derived cells (EPDC), and murine cardiomyocyte-like cells (HL-1), both under normal culture conditions and in "simulated ischemia" (1% O_2, serum and glucose deprivation) (Figure 4).

On DeAM + E, HL-1 cells adhered better within the first 30 min, but no further increase in adhesion was observed during longer cultivation periods (Figure 4a). In contrast, EPDCs (Figure 4b) showed improved adhesion capacity on DeAM + E only after 120 min. Human cardiac fibroblasts (hCF) (Figure 4c) displayed the trend towards increased adhesion on DeAM + E ($p = 0.07$).

Culturing on DeAM + E reduced cell death for all tested cell types under normoxic conditions (Figure 4d–f). Under "simulated ischemia" conditions, necrosis of HL-1 cells substantially decreased when cultured on DeAM + E (Figure 4g). In the case of EPDCs exposed to "simulated ischemia", this effect was reversed, despite remarkable minimization of LDH-release on both surfaces compared to standard cell culture conditions (normalized to value 1). In addition, hCF also benefited from culturing on DeAM + E under "simulated ischemia" conditions and displayed less cell necrosis (Figure 4i).

The cell growth rate was improved on DeAM + E for all cell types as seen by BrdU incorporation in HL-1 cells, EPDCs, and hCF, both under normoxia and in "simulated ischemia" (Figure 4j–o), highlighting the dominant advantage of the modified scaffold provided by DeAM + E.

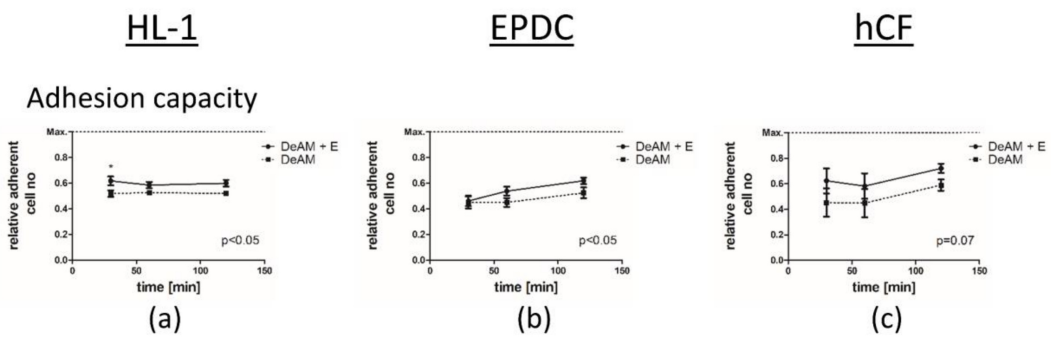

Figure 4. *Cont.*

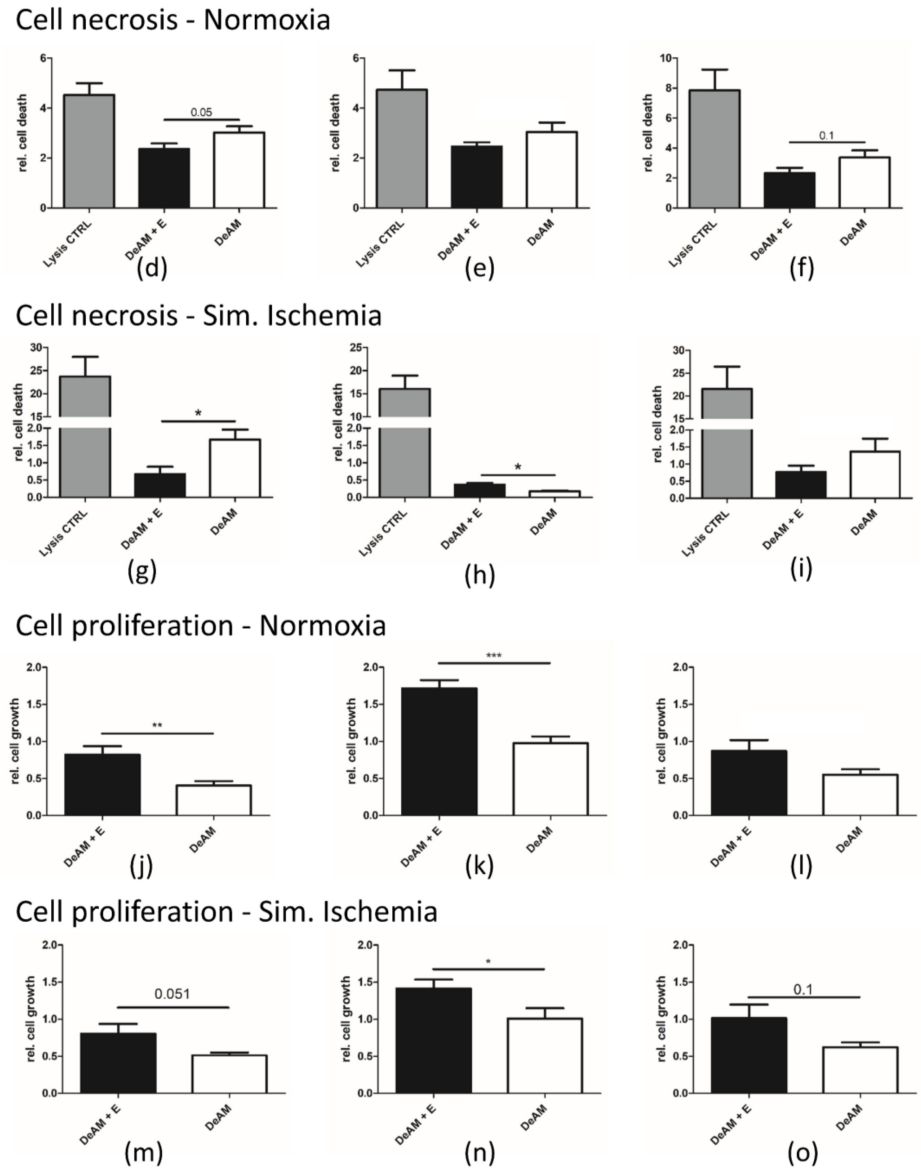

Figure 4. Interaction and viability of HL-1 cells, EPDCs and hCF cultured on DeAM and DeAM + E scaffolds. Adhesion capacity of contractile (**a**) HL-1 cells, (**b**) EPDCs and (**c**) hCF was determined via calcein staining on DeAM (dotted line) and DeAM + E (solid line). Cell necrosis was determined by measuring LDH release of HL-1 cells, EPDCs and hCF under normoxia (**d**–**f**) and "simulated ischemia" (**g**–**i**) cultured on DeAM + E (black) and DeAM (white). Lysis control (grey) indicates total cell death. Cell growth was determined by measuring BrdU-incorporation of HL-1 cells, EPDCs and hCF under normoxia (**j**–**l**) and "simulated ischemia" (**m**–**o**) cultured on DeAM + E (black) and DeAM (white). * $p < 0.05$, ** $p < 0.01$, *** $p < 0.001$; $n \geq 3$.

2.5. Coating with hgECM Modulates Inflammatory Responses

2.5.1. Pro-inflammatory Cytokine Release

Inflammation plays an exceedingly important role in myocardial remodeling as well as in spontaneous and induced regeneration processes. Any biologic implant must be able to balance pro- and anti-inflammatory stimuli to exert appropriate and sustained functional effects. We therefore studied the effect of DeAM, hgECM coated DeAM on the pro- and anti-inflammatory cytokines IL-6,

TNF-α, and IL-10 secreted from human peripheral blood mononuclear cells (PBMCs), and monocytes as well as $CD14^+$-derived macrophage subpopulations (Figure 5).

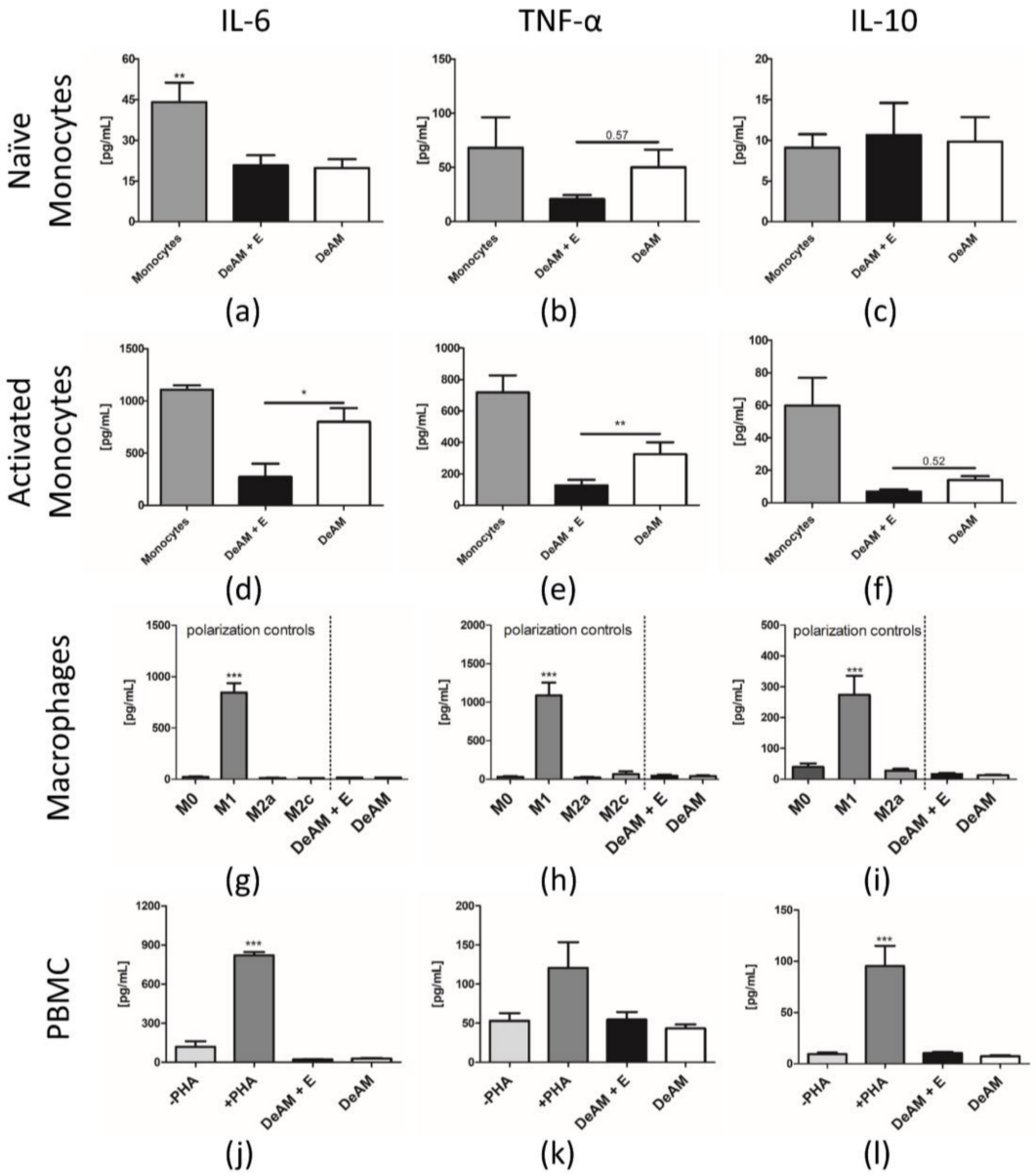

Figure 5. Cytokine release from monocytes, macrophages and PBMCs cultured on DeAM and DeAM + E scaffolds determined by ELISA. Supernatants were collected after 24 h of naïve ((**a**–**c**) ** $p < 0.01$ to all groups) and LPS-activated ((**d**–**f**) * $p < 0.05$, ** $p < 0.01$) CD14+ monocytes on DeAM + E (black), DeAM (white) or monocyte standard culture control conditions (grey). Macrophages derived from $CD14^+$-monocytes (M0) were polarized towards pro-inflammatory M1- and anti-inflammatory M2a- and M2c-type. After 2 days, supernatants were collected and analyzed for IL-6, TNF-α and IL-10 ((**g**–**i**) *** $p < 0.001$ to all groups) concentration. PBMCs from human buffy coat were cultured for 5 days. Supernatants were collected and analyzed for cytokine secretion of IL-6, TNF-α and IL-10 ((**j**–**l**) *** $p < 0.001$ to all groups). The positive control group was stimulated with PHA. $n \geq 3$.

Compared to standard culture plate conditions, cytokine secretion of naïve monocytes was affected by DeAM both with and without hgECM coating. IL-6 secretion was significantly decreased on both surfaces (Figure 5a) but the release of TNF-α (Figure 5b) was reduced only in monocytes cultured

on DeAM + E. The secretion of IL-10 was unchanged on either surface (Figure 5c). Lipopolysaccharide (LPS)-activated monocytes demonstrated a marked suppression in the secretion of IL-6 (Figure 5d) and TNF-α (Figure 5e) on DeAM + E. However, no difference in IL-10 secretion was observed in the presence of DeAM + E or DeAM (Figure 5f).

Macrophages derived from M-CSF stimulated $CD14^+$ monocytes once polarized towards the pro-inflammatory M1 type were unequivocally identifiable by a substantial increase in all measured cytokines IL-6, TNF-α and IL-10 (Figure 5g–i) compared to all control groups as well as macrophages cultured on DeAM and DeAM + E. Thus, polarization towards pro-inflammatory M1 type on DeAM as well as DeAM with additional hgECM coating did not occur. Because IL-10 stimulation was used to induce M2c polarization, IL-10 secretion by the M2c control could not be determined (Figure 5i).

The cytokine secretion profile of PBMCs demonstrated clearly that only the Phytohemagglutinin (PHA) stimulated PBMC (positive control) secreted significantly more IL-6, TNF-α and IL-10 (Figure 5j–l) than all other groups including PBMCs cultured on both DeAM and DeAM + E. Therefore, the cytokine secretion profiles of cultured PBMCs were not stimulated by DeAM or DeAM + E.

2.5.2. Macrophage Polarization and T Cell Proliferation

Finally, we examined the impact of hgECM coating on macrophage polarization towards the M1 or M2 type by examining the magnitude of surface marker expression. In general, ECM has the potential to induce M2 polarization [19] and might also influence T cell proliferation. Therefore, we tested the behavior of macrophages and T cells in contact with the patch materials. Immunophenotyping (CD surface antigens) and proliferation by Carboxyfluorescein Succinimidyl Ester (CFSE) staining was determined by flow cytometry (Figure 6).

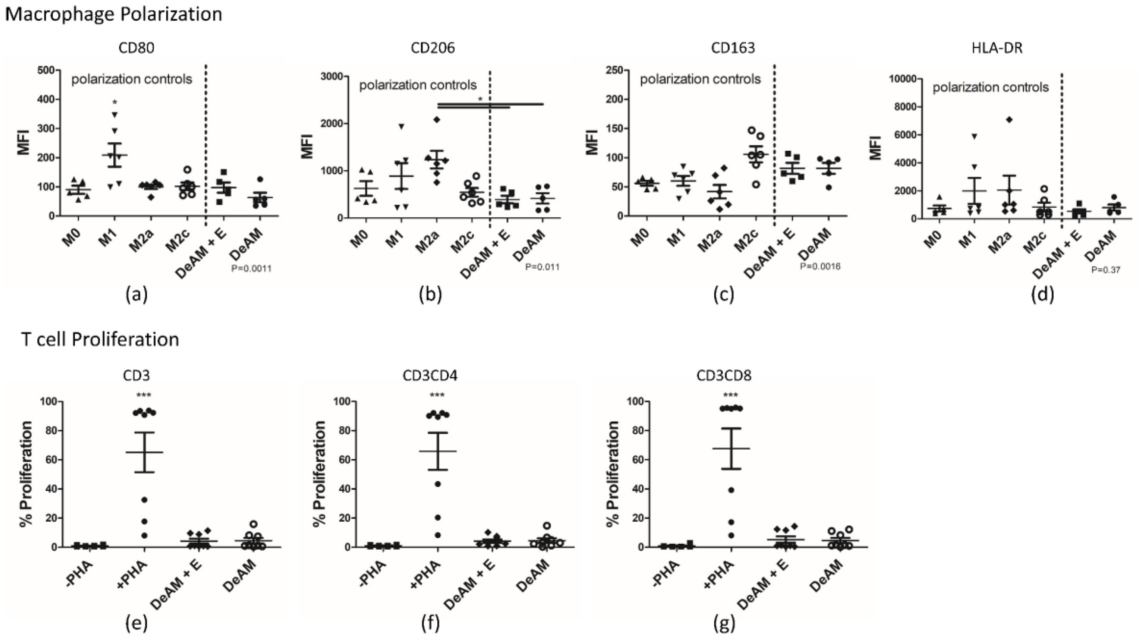

Figure 6. Polarization of M0 macrophages towards the pro-inflammatory M1 and anti-inflammatory M2a and M2c type was determined by flow cytometry after culturing for 48 h on DeAM + E and DeAM. Mean fluorescence intensities (MFI) for (**a**) CD80 (* $p < 0.05$ to all groups); (**b**) CD206; (**c**) CD163 and (**d**) HLA-DR marker expression are depicted. Polarization control groups (M0, M1, M2a, M2c) were cultured on standard plastic surface. PBMC were labeled with CFSE and cultured for 5 days on DeAM and DeAM + E. Proliferation was determined by flow cytometry for (**e**) $CD3^+$; (**f**) $CD3CD4^+$ and (**g**) $CD3CD8^+$ T cells (*** $p < 0.001$ to all groups). Negative (−PHA) and positive stimulated (+PHA) controls were cultured on standard culture surface, $n \geq 5$.

After macrophage polarization, the M1 macrophage polarization control group represents the pro-inflammatory positive control and displayed upregulated expression of the CD80 marker (Figure 6a). The anti-inflammatory control groups M2a and M2c expressed predominantly CD206 (Figure 6b) and CD163 (Figure 6c) and on higher levels, respectively. Although expected to be highly expressed in M1 macrophages, HLA-DR (Figure 6d) did not significantly differ between control groups and amniotic scaffolds. Macrophages cultured on DeAM or DeAM + E showed a similar expression profile. In both M2 control groups as well as the M0 control group, no upregulation of CD80 was observed. Similar to the M2c control, macrophages on both surfaces showed the trend of higher expression of CD163 and no change in CD206 expression, suggesting that an M2c polarization took place.

As expected, PHA-stimulation of PBMCs induced a substantial increase in the proliferation of $CD3^+$ T cells as well as with a comparable proportion in the $CD4^+$ and $CD8^+$ T cell subpopulations (Figure 6e–g). In contrast, culture on DeAM and DeAM + E scaffolds alone did not induce a significant proliferation of T cells.

3. Discussion

In the present work, we show that ECM isolated from human myocardium has the potential to modify the regenerative properties of a biological scaffold—decellularized human amniotic membrane—so that it is potentially better suited for therapeutic application in the diseased heart.

ECM has recently been shown to have great potential in regenerative and differentiation-guiding characteristics. Specific and crucial tissue characteristics are determined by the unique multi-protein composition of the ECM [20]. It is primarily produced by fibroblasts, and its unique biological properties can vary in response to physical changes. In the heart, ECM plays an essential role in myocardial infarction and other pathologies leading to heart failure [21]. Cardiac ECM has been isolated from different species, such as zebrafish [22], cow [23], rat [24] or pig [25], and is deemed a promising source of organ-specific, multi-protein preparations for intramyocardial or epicardial application. ECM also supports an anti-inflammatory response [26–28] and induces specific gene expression [29,30]. Processing of the naïve decellularized ECM to microparticles, followed by reconstitution to a hydrogel, widens the potential application range [31] and has been shown to be feasible [32] and translatable for cardiac tissue [33].

The use of animal tissue for experimental and clinical ECM applications is well established [10,23,25]. For example, cardiac ECM from Zebrafish was processed into microparticles to enable in vivo analyses by intramyocardial injection [22]. Porcine ECM from different organs, processed to a hydrogel, was shown to hold the potential to induce cardiac remodeling and increase cardiac function in large animal models [33]. However, the possibilities of applying human material have been less thoroughly researched. For instance, Godier-Furnémont et al. explored the possibility to design a patch with human ECM slices, but the addition of fibrin glue was necessary to stabilize the patch [12]. Moreover, the dimensions of an intact ECM slice were limited by the size of the available source myocardium. In contrast, our approach allows the use of human cardiac ECM to completely cover a sizable scaffold material, facilitating future clinical applications. We have previously shown that hcECM induces selectively cardiac differentiation/maturation and is cytoprotective for cardiomyocytes as well as stem and progenitor cells [13,14]. However, because it is a very fragile substance, it requires a mechanically stable scaffold material for application onto or into the heart. Therefore, ECM homogenization is a critical additional processing step that could open up new possibilities in regenerative medicine [34]. Additionally, we have already been able to show that processing the human cardiac ECM in this way does not impact its cytoprotective capacity [15].

Previous attempts to improve the biologic function of scaffold materials were largely made using standardized proteins such as gelatin [11] or fibrin [35]. More recently, Faulk et al. demonstrated the feasibility of covering polypropylene mesh scaffold with porcine dermal ECM [31]. However, using a

polymer-based scaffold material in the heart risks inducing pro-inflammatory reactions, and therefore graft rejection, due to its chemical composition [8].

To avoid the potential complications accompanying the use of a synthetic scaffold material, we decided to use DeAM as an ECM scaffold which, in its naive form, we previously tested in vivo [6]. Therefore, the additional coating of hgECM does not dramatically change the characteristics of the resulting composite material, but, ideally, simply adds cardiac specificity. In line with this hypothesis, we did not observe a difference in the mechanical properties of coated and uncoated DeAM. While artificial polymer materials in general react linearly [5], the amniotic membrane can compensate a certain amount of stress by its natural flexibility, later followed by a linear elastic behavior until it reaches the maximum stress/strain slope. Material stiffness can also have a significant impact on cell behavior [36,37] but it is not affected by hgECM coating. Additionally, we were concerned about the biologic activity of the myocardial ECM product in terms of lineage support and cytoprotection which is most likely determined by its tissue-specific protein composition [14]. By mass spectrometry, we identified ECM proteins such as chitinase, a participant in pathogen defense and preventer of apoptosis by AKT activation, the Myosin binding protein C, involved in filament binding and muscle contractions, and the protein ecdysoneless homolog, which regulates p53 stability. Even though it remains unclear how ECM precisely exerts its cytoprotective effects, the presence of those partly intracellular proteins support the objective that coating of DeAM with hgECM increases cell proliferation and reduces cell necrosis as well as pro-inflammatory cytokine secretion. We observed that monocytes were not activated and secreted less IL-6 and TNF-α if cultured on coated scaffold in an activated state, suggesting the potential to ameliorate the inflammation present in infarcted myocardium.

In addition, according to our expectations both tested scaffolds did not induce a pro-inflammatory macrophage reaction (i.e., M1 polarization) but rather trend to induce a polarization towards the anti-inflammatory M2-type. The kind of material has a sensitive effect on the macrophage polarization behavior. It was shown that an electrospun polymer could induce a polarization towards the pro-inflammatory M1-type [8,27] whereas the introduction of collagen [38] or ECM [27] into the scaffold design reduced or even reversed that effect. Moreover, Ariganello et al. [39] highlights in particular decellularized pericardial tissue being supportive for guiding macrophage polarization towards anti-inflammatory tissue-remodeling state underlining the beneficial impact of additional hgECM coating.

We primarily aim at using the DeAM + E composite material for sustained delivery of biologics (cell products, reprogramming factors etc.) to the epicardial surface of the infarcted heart, since the epicardium is known to be highly involved in cardiac regeneration processes. In zebrafish and young mice, it has been shown that the epicardium can completely regenerate the infarcted myocardium [2,40,41]. To support cardiac regeneration via the epicardium, patches with cellular and protein-based [35,42] or polymeric [5,11,43] background have been designed by other groups. Epicardial cells were shown to have regenerative and angiogenic potential not only in animals but also when isolated from human hearts [44]. We are convinced that the limited regenerative capacity of the human heart can be augmented by tailored epicardial patch designs.

In summary, we developed a cell-free human amniotic membrane/myocardial ECM composite scaffold material with favorable in vitro biological and mechanical properties that has the potential be used in large animal experiments and ultimately clinical studies. As a cell-free material, the production process can readily be scaled-up under GMP conditions. Further in vivo testing will reveal whether the DeAM + E material alone is able to significantly modify post-infarct remodeling processes. In any event, it may serve as a universal platform for epicardial delivery of a broad spectrum of cells and therapeutic agents.

4. Material and Methods

4.1. Tissue Source

Left ventricular myocardium was collected from explanted hearts from patients who underwent heart transplantation for end-stage dilated cardiomyopathy. All patients were in New York Heart Association class II or IV, with a left ventricular ejection fraction <20%, and were not on mechanical circulatory support. Hepatitis B or C and HIV infection were ruled out preoperatively. The study protocol conforms to the ethical principles outlined in the Declaration of Helsinki. Patients provided informed consent for the use of the tissue for research purposes, and the process of tissue collection was approved by the Institutional Review Board and ethics committee of Charité—Universitätsmedizin Berlin (EA4/028/12, 20 June 2012).

Human full term placentas (n = 17) were anonymously obtained after cesarean delivery of healthy and uncomplicated pregnancies from women who had given written informed consent for use of the placenta for research purposes.

4.2. Human Amniotic Membrane Processing

Excess blood was removed by washing with Hank's balanced salt solution (HBSS; Life Technologies, Carlsbad, CA, USA. The amniotic membrane (AM) was mechanically peeled from the underlying chorion and washed several times in HBSS to remove blood. Subsequently, AM was washed with phosphate buffered saline without calcium and magnesium ($PBS^{-/-}$, Life Technologies) and placed in lysis buffer (10 mM Tris and 0.1% EDTA (both Carl-Roth, Karlsruhe, Germany) for 1 h at room temperature, followed by incubation in 0.5% sodium dodecyl sulfate (SDS; Carl-Roth) solution for 4 h at room temperature with constant stirring. Next, the AM was washed in PBS three times at room temperature and finally overnight at 4 °C under constant agitation.

Decellularized AM (DeAM) was cut into appropriate pieces and lyophilized.

4.3. ECM Processing

Human myocardium was harvested under sterile conditions and stored for no longer than 48 h at 4 °C before sectioning. Human Cardiac Extracellular Matrix (hcECM) isolation and processing was performed as described [45]. The myocardium was cut into cubes with an edge length of approximately 1 cm, embedded into Tissue Tec O.C.T (Sakura Inc., Alphen aan den Rijn, The Netherlands), sectioned in 300 µm thick slices using a CM 3050S cryostat (Leica, Wetzlar, Germany), and stored at −80 °C before further processing. Subsequently, tissue slices were shaken for 2 h with lysis buffer (10 mM Tris, 0.1% w/v EDTA, pH 7.4; Carl-Roth) followed by SDS (0.5% w/v in PBS; Carl-Roth) incubation for 6 h under constant agitation at room temperature. Then, the slices were washed three times with PBS for 10 min to remove SDS, followed by an overnight washing period with Dulbecco's phosphate buffered saline (DPBS) including 100 U/mL penicillin/streptomycin and nystatin to guarantee complete removal of SDS. Finally, the tissue was immersed in fetal bovine serum (FBS; Biochrom, Cambridge, UK) for 3 h at 37 °C followed by three washes with DPBS/penicillin/streptomycin/nystatin for 10 min each. Prior to further processing and/or experimentation, cECM slices were stored at 4 °C for up to 2 weeks.

To process decellularized matrix, slices were snap-frozen in liquid nitrogen, lyophilized and pulverized using the Precellys ceramic Kit 1.4 mm (PEQLAB Biotechnologie, Erlangen, Germany) and the Minilys homogenizer (PEQLAB Biotechnologie) at a rate of six runs per 1 min at 4000 rpm. Resulting particles were resolved in distilled water and filtered using a 200 µm transfusion filter system to remove larger particles, lyophilized again for 48 h, and stored at −80 °C. For homogenization, 1 mg/mL pepsin from porcine gastric mucosa (Sigma-Aldrich, Saint Louis, MO, USA) was dissolved in 0.01 M HCl, and incubated with 10 mg/mL hcECM particles for 48 h under constant agitation. To inhibit the Pepsin activity, the hcECM solution was neutralized on ice and brought to physiological pH by adding pre-cooled 10× PBS and 0.1 M NaOH. Finally, the concentration was set to 8 mg/mL

by dilution using 1× PBS and hcECM Hydrogel (hgECM) was stored at 4 °C for not longer than 24 h before use.

4.4. Preparation of hgECM Coated Composite Materials

With an 8 mm Biopsy-Punch (PFM Medical, Cologne, Germany), the DeAM was cut into discs and lyophilized. One disc of DeAM was placed into each well of a 48-well plate and held in place by rings cut from silicone tubing (Ismatec, Wertheim, Germany) providing an inner diameter equal to 96-well format, and washed with PBS. The samples were completely coated by adding 150 µL/cm^2 hgECM solution and dried for 48 h at 37 °C in a non-humidified incubator. After two gentle washes with PBS, the coated membranes were used for experiments. DeAM and DeAM coated with hgECM (DeAM + E) were tested.

4.5. Scanning Electron Microscopy

Samples were washed twice in PBS and fixed with 2.5% grade I glutaraldehyde (Sigma-Aldrich) for 30 min at room temperature. Subsequently, samples were washed again in PBS and dried using 5 min incubation steps in increasing Ethanol (Carl-Roth) concentration (mixed with ddH_2O) (30%, 50%, 70%, 80%, 90%, 95%) followed by two final incubations in 100% Ethanol. Ethanol was removed by two incubations in Hexamethyldisilazane (Sigma-Aldrich) for 10 min each. Samples were air-dried overnight under a fume hood. Then, samples were placed on a stamp (Agar Scientific, Essex, UK) with 12 mm PLANO Tab (Plano GmbH, Wetzlar, Germany) and sputter coated with gold for 30 s (JFC-1200 Fine Coater; JEOL). Finally, samples were imaged using the JCM 6000 benchtop SEM (JEOL, Tokyo, Japan) in high vacuum mode at 10 kV.

4.6. Mechanical Testing of Amniotic Membrane Stress Measurement

Uniaxial pulling tests were performed in a wet state for the different groups under a BOSE testing bench (BOSE ElectroForce® TestBench, TA Instruments, New Castle, DE, USA) using fixed clamps. Sample length was set to 1 cm, while thickness and width were individually measured using a micrometer (precision: ±0.001 µm) and a caliper (precision: ±0.01 mm) (Mitutoyo Corporation, Kawasaki, Japan), respectively. Crosshead speed was set to 0.05 mm/s and pulling up to 0.9 strain. Elastic moduli were calculated as the slope of the most linear region presented on the stress over strain curve. Stress and strain were obtained in agreement with the initial cross sectional area and length of each sample. Maximum stress was obtained as the maximum load before sample rupture.

4.7. Mass Spectrometry

The hgECM (140 µg) was resolved in 40 µL P-buffer (0.05 M Tris Base pH 7.5 (Sigma-Aldrich), 0.05 M potassium chloride (Merck, Darmstadt, Germany), 0.11 M Chaps (SERVA, Heidelberg, Germany), 20% glycerine (Merck), PhosSTOP (Roche, Basel, Switzerland), cOmplete (Roche)) and sonicated on ice. Then, 200 µL UA (0, 1 M Tris HCL pH 8.5 (Sigma-Aldrich) and 8 M Urea (Sigma-Aldrich)) were added and incubated for 10 min at room temperature. The solution was transferred into an amicon filter (10 kDa cut off, Merck), followed by buffer exchange to trypsin solution, (12 µg trypsin in 50 mM ammonium bicarbonate; Promega, Madison, WI, USA) and incubated at 37 °C overnight. Subsequently, ABC-buffer (50 mM ammonium bicarbonate; Sigma-Aldrich) was added and the solution centrifuged for 10 min at 14,000 rpm at room temperature. The flow-through was desalted using ZipTip C18 (Merck) pipet tips according the manufacturer's protocol. Peptide samples were dried in a SpeedVac (Thermo-Fisher, Waltham, MA, USA) concentrator and extracted afterwards in 20 µL 0.1% trifluoroacetic acid (TFA) for 15 min at room temperature. Analysis was performed using UPLC (Dionex Ultimate 3000, Thermo-Fisher) ESI-QTOF-mass spectrometer (Imapct II, bruker daltonics, Billerica, MA, USA). Mass spectra were evaluated using MASCOT software (version number 2.2, Matrix Science, Boston, MA, USA) automatically searching the SwissProt 51.9 database (Human 553474 sequences; 198069095 residues, Cambridgeshire, UK). MS/MS ion

search was performed with the following set of parameters: (i) taxonomy: *Homo sapiens* (human) (20175 sequences); (ii) proteolytic enzyme: trypsin; (iii) maximum of accepted missed cleavages: 1, (iv) mass value: monoisotopic, (v) peptide mass tolerance 10 ppm; (vi) fragment mass tolerance: 0.05 Da; and (vii) variable modifications: oxidation. No fixed modifications were considered. Only proteins with scores corresponding to $p < 0.05$ were considered. The cut-off score for individual peptides was equivalent to $p < 0.05$ for each peptide as calculated by MASCOT (version number 2.2).

4.8. Cell Culture

All cell types were negatively tested for mycoplasma contamination.

4.8.1. HL-1

Murine HL-1 cardiomyocytes (HL-1), immortalized using the simian virus SV40 T-antigen under the control of an atrial natriuretic factor (ANF) promotor [46], were generously provided by William C. Claycomb (Louisiana State University, New Orleans, LA, USA) and used at passages 18–44. Cells were cultured in Claycomb medium with 10% HL-1 Cell Screened FBS (Merck), 100 U/mL penicillin, 100 µg/mL streptomycin, 2 mM L-Glutamine (Gibco, Waltham, MA, USA) and 100 µM norepinephrine, and cultured on 0.02% gelatin/5 µg/mL fibronectin-coated (Sigma-Aldrich) cell culture flasks at 37 °C and 5% CO_2.

4.8.2. Human Cardiac Fibroblasts

Human cardiac fibroblasts (hCF; generously donated by S. van Linthout, BCRT, Berlin) were cultured in DMEM (Gibco), 10% FBS (Biochrom) added and 100 U/mL penicillin, 100 µg/mL streptomycin (Gibco).

4.8.3. Human Immune Cells

Human immune cells (monocytes, macrophages and peripheral blood mononuclear cells) were cultured in VLE RPMI 1640 Medium (Biochrom), 10% hAB Serum (Sigma-Aldrich) 100 U/mL penicillin, 100 µg/mL streptomycin and 2 mM L-Glutamine (Gibco).

Peripheral blood mononuclear cells (PMBCs) were isolated from Buffy Coat (bought from Deutsches Rotes Kreuz with approval by the Institutional Review Board and ethics committee of Charité—Universitätsmedizin Berlin EA1/372/16) using Biocoll (Biochrom) density gradient.

Monocytes were isolated from PMBCs using the $CD14^+$ Magnetic Cell Separation kit (Miltenyi Biotec, Bergisch Gladbach, Germany).

Macrophages were differentiated from isolated monocytes by a 7 day incubation in culture medium with 50 ng/mL M-CSF (Miltenyi Biotec) and collected with a cell scraper.

4.8.4. Epicardial Derived Cells

Adult human atrial samples (auricles) were obtained during cardiac surgery as redundant material anonymously collected as surgical waste under general informed consent. Epicardial Derived Cells (EPDC) were isolated from human heart auricles as described [44]. Briefly, the epicardial layer was peeled off with sterile tweezers and incubated for 30 min in Trypsin/EDTA at 37 °C. Cells were separated with a cell strainer and cultured in a 1:1 mixture of Dulbecco's modified Eagle's medium (DMEM-glucose low; Invitrogen, Carlsbad, CA, USA) and Medium 199 (M199; Invitrogen) supplemented with 10% heat-inactivated FBS (Biochrom), 100 U/mL penicillin/streptomycin (Gibco) and 5 ng/mL TGFβ (EUROFINS) on 0.1% gelatin coated cell culture dish.

4.9. Simulated Ischemia

Simulated ischemia cells were cultured on patch material or cell culture dishes for 24 h before being exposed to glucose/serum deprivation (glucose- and FBS-free DMEM (Thermo-Fisher)), with 100 U/mL penicillin/streptomycin (Gibco), 1% O_2/5% CO_2) for 5 h in a Binder CB150 incubator (CB150, Binder, Tuttlingen, Germany).

4.10. Cell Behavior

4.10.1. Cardiac Cell Adhesion

Cells were labelled with 5 µM Calcein (MoBiTec, Herrljunga, Sweden) following the manufacturer's instructions. For determining adhesion rates, 125,000 HL-1 cells, or 20,000 hCF or EPDCs per cm^2 were used. Cells were placed onto the scaffolds and incubated at 37 °C for 30 min, 60 min, or 120 min. Supernatants containing unbound cells were collected and cells were lysed with a final concentration of 1 °C% Triton-X100. Fluorescence intensity, representing the number of cells, was analyzed using the MithrasLB940 plate reader (Berthold Technologies, Bad Wildbad, Germany. Adherent cell number was calculated via comparison to a defined cell number standard, and the amount of adherent cells was determined.

4.10.2. Necrosis (LDH)

Determination of cell necrosis was performed by measuring the release of Lactate Dehydrogenase (LDH) using the CytoTox-ONE™ Homogeneous Membrane Integrity Assay (Promega). Then, 125,000 HL-1 cells, or 20,000 hCF, or EPDCs per cm^2, were cultured onto the scaffolds or on standard cell culture conditions for controls. Cells were either cultured on standard culture conditions for 24 h or additionally exposed to simulated ischemia. Next, supernatants were analyzed for LDH release according to manufacturer's instructions, and fluorescence was measured using the MithrasLB940 plate reader (Berthold Technologies). Results were normalized to normal cell culture conditions.

4.10.3. Cell Growth

Cell growth was analyzed using the BrdU Cell Proliferation ELISA Kit (Roche). To determine cell growth, 62,500 HL-1 cells, or 20,000 hCFs or EPDCs per cm^2 were cultured onto the scaffolds or standard cell culture conditions as controls. Cells were cultured under standard conditions for 24 h at 37 °C in a humidified incubator. Subsequently, labelling reagent was added and incubated for 5 h at 37 °C under normoxia or simulated ischemia. Afterwards, cells were analyzed for BrdU-incorporation according to protocol. Finally, the reaction was stopped by adding 1 M H_2SO_4, and 100 µm of the solution was transferred to a fresh 96-well plate. Read out was performed using the SpectraMax 340PC384 (Molecular Devices, San Jose, CA, USA).

4.11. Immunological Analyses

4.11.1. Monocytes–Cytokine Secretion

To determine cytokine secretion, 100,000 monocytes were cultured onto patch materials and incubated for 24 h at 37 °C. For the positive control, medium was supplemented with 200 ng/mL Lipopolysaccharide (LPS). Supernatants were collected and cytokine secretion was detected using Human ELISA MAX™ Deluxe Kits (Thermo-Fisher) for IL-6, IL-10 and TNF-α following the manufacturer's protocol.

4.11.2. Staining Procedure for Flow Cytometry

Cells were collected and washed once in buffer (PBS, 1% FBS (Biochrom), 0.5% Sodium azide (Carl-Roth)). The supernatant was discarded completely and 50 µL staining solution in buffer containing all labeling antibodies was added and incubated for 30 min at 4 °C.

Subsequently, the suspension was washed once with buffer and suspended in buffer containing 1% Paraformaldehyde (PFA, Carl-Roth) and analyzed the next day. The following antibodies were used for macrophage staining: CD163-Fitc (1:20, BioLegend, San Diego, CA, USA), CD80-PE (1:20, BioLegend), CD16-PerCPCy5.5 (1:200, BioLegend), CD206-APC (1:100, BioLegend), CD14-APCCy7 (1:100, BD, Franklin Lakes, NJ, USA), HLA-DR-PeCy7 (1:400, BioLegend), Life/Dead-V510 (1:100, Thermo-Fisher). Following antibodies were used for T cell staining in the proliferation setup: CD8-PE (1:50, Miltenyi Biotec), CD4-APC (1:100, BioLegend), CD3-APCCy7 (1:100, BioLegend).

4.11.3. Peripheral Blood Mononuclear Cell Cytokine Secretion and T Cell Proliferation

CFSE stain for T cell proliferation was performed using the CFSE labeling procedure from the Total Cytotoxicity & Apoptosis Detection Kit (Biomol, Hamburg, Germany). Briefly, PBMCs (provided by Karen Bieback; Heidelberg) were adjusted to 1×10^7 cells in 1 mL assay buffer, washed twice in assay buffer and a labeled 200 µL CFSE working solution was added to 1.8 mL cell suspension in assay buffer. The labeled suspension was incubated for 15 min at room temperature. The reaction was stopped by adding medium followed by two washing steps with assay buffer. Finally, cells were suspended in the medium and used for the experiment. Then, 150,000 PBMCs were cultured on patch materials for 5 days. The positive control medium was supplemented with 5 µg/mL Phytohaemagglutinin (PHA). Subsequently, cells were harvested and analyzed for proliferation of $CD3^+$, $CD3CD4^+$ and $CD3CD8^+$ T cell proliferation by flow cytometry (gating strategy is provided in supplementary material Figure S2). Supernatants were collected and cytokine secretion was detected using Human ELISA MAX™ Deluxe Kits (Thermo-Fisher) for IL-6, IL-10 and TNF-α following the manufacturer's protocol.

4.11.4. Macrophage Polarization

To investigate macrophage polarization, 100,000 macrophages were cultured for 48 h on patch materials or cell culture dishes. To induce polarization towards M1, the culture medium was supplemented with 20 ng/mL INFy +100 ng/mL LPS. For M2a polarization, 20 ng/mL IL-4 and for M2c 20 ng/mL IL-10 was used.

After 2 days of culture, supernatants were collected for detection of cytokine secretion via ELISA using Human ELISA MAX™ Deluxe Kits (Thermo-Fisher) for IL-6, IL-10 and TNF-α following the manufacturer's protocol. Cells were harvested using Accutase (Innovative Cell Technologies, San Diego, CA, USA)) and analyzed for polarization marker expression by flow cytometry (gating strategy is provided in supplementary material Figure S1).

4.12. Statistics

Data are shown as mean ± SEM. Comparisons passed normality and equal variance testing before the significance was tested. Differences between more than two groups were determined by one-way ANOVA with Bonferroni *t*-test for multiple comparisons. For two-group comparisons, a two-tailed student's *t*-test was performed if the normality test was passed. The Mann-Whitney test was performed if non-normality was detected. Changes over time were tested by two-way ANOVA with Bonferroni's correction. GraphPad Prism v. 5.03 (GraphPad, La Jolla, CA, USA) was used for data analysis and plotting. A *p*-value of $p < 0.05$ was considered significant.

5. Conclusions

The source and composition of applied extracellular matrix is crucial for specific application. Here, we demonstrated the additional coating of cell-free amniotic membrane scaffolds with processed human cardiac extracellular matrix. The novel resulting patch material not only specifically supports the culture and interaction of cardiac cells such as cardiomyocytes, epicardial cells, and cardiac fibroblasts, but also exerts immunomodulatory effects on cell subsets relevant for cardiac regeneration and tissue engineering. The newly designed patch system may therefore enhance

the therapeutic capacity of epicardial composite materials and pave the way for improved cardiac regeneration attempts.

Supplementary Materials: Supplementary materials can be found at http://www.mdpi.com/1422-0067/19/4/1032/s1.

Acknowledgments: We would like to acknowledge the assistance of the BCRT Flow Cytometry Lab, Karen Bieback from the Institute of Transfusion Medicine and Immunology, Ruprecht-Karls University of Heidelberg, Mannheim, Germany for providing human immune cells and Sophie van Linthout from the Berlin-Brandenburg Center for Regenerative Therapies for providing human cardiac fibroblasts. We thank Olivia Reidell for copy-editing this manuscript. This work was supported by the Federal Ministry of Education and Research and the federal states of Berlin and Brandenburg [FKZ 13GW0099]. We acknowledge support from the German Research Foundation (DFG) and the Open Access Publication Fund of Charité—Universitätsmedizin Berlin.

Author Contributions: Matthias Becker: Conception and design of the work, acquisition, analysis and interpretation of data, writing the manuscript; Janita A. Maring: Interpretation of Data, substantively revised the work; Maria Schneider: Interpretation of Data; Aarón X. Herrera Martín: Acquisition and analysis of data; Martina Seifert: Interpretation of Data, substantively revised the work; Oliver Klein: Acquisition of data; Thorsten Braun: Acquisition of data; Volkmar Falk: Substantively revised the work; Christof Stamm: Drafted and substantively revised the work.

Conflicts of Interest: The authors declare no conflict of interest.

Abbreviations

ECM	extracellular matrix
hcECM	human cardiac extracellular matrix
hgECM	human cardiac extracellular matrix hydrogel
AM	amniotic membrane
DeAM	decellularized amniotic membrane
DeAM + E	decellularized amniotic membrane coated with human cardiac extracellular matrix hydrogel
PBMCs	peripheral blood mononuclear cells

References

1. Roger, V.L.; Go, A.S.; Lloyd-Jones, D.M.; Benjamin, E.J.; Berry, J.D.; Borden, W.B.; Bravata, D.M.; Dai, S.; Ford, E.S.; Fox, C.S.; et al. Heart Disease and Stroke Statistics—2012 Update. *Circulation* **2012**, *125*, e2–e220. [PubMed]
2. Porrello, E.R.; Mahmoud, A.I.; Simpson, E.; Hill, J.A.; Richardson, J.A.; Olson, E.N.; Sadek, H.A. Transient regenerative potential of the neonatal mouse heart. *Science* **2011**, *331*, 1078–1080. [CrossRef] [PubMed]
3. Hastings, C.L.; Roche, E.T.; Ruiz-Hernandez, E.; Schenke-Layland, K.; Walsh, C.J.; Duffy, G.P. Drug and cell delivery for cardiac regeneration. *Adv. Drug Deliv. Rev.* **2015**, *84*, 85–106. [CrossRef] [PubMed]
4. Smith, R.R.; Marbán, E.; Marbán, L. Enhancing retention and efficacy of cardiosphere-derived cells administered after myocardial infarction using a hyaluronan-gelatin hydrogel. *Biomatter* **2013**, *3*, e24490. [CrossRef] [PubMed]
5. Gu, X.; Matsumura, Y.; Tang, Y.; Roy, S.; Hoff, R.; Wang, B.; Wagner, W.R. Sustained viral gene delivery from a micro-fibrous, elastomeric cardiac patch to the ischemic rat heart. *Biomaterials* **2017**, *133*, 132–143. [CrossRef] [PubMed]
6. Roy, R.; Haase, T.; Ma, N.; Bader, A.; Becker, M.; Seifert, M.; Choi, Y.-H.; Falk, V.; Stamm, C. Decellularized amniotic membrane attenuates postinfarct left ventricular remodeling. *J. Surg. Res.* **2016**, *200*, 409–419. [CrossRef] [PubMed]
7. Tomecka, E.; Wojasinski, M.; Jastrzebska, E.; Chudy, M.; Ciach, T.; Brzozka, Z. Poly(l-lactic acid) and polyurethane nanofibers fabricated by solution blow spinning as potential substrates for cardiac cell culture. *Mater. Sci. Eng. C* **2017**, *75*, 305–316. [CrossRef] [PubMed]
8. Castellano, D.; Blanes, M.; Marco, B.; Cerrada, I.; Ruiz-Sauri, A.; Pelacho, B.; Arana, M.; Montero, J.A.; Cambra, V.; Prosper, F.; et al. A comparison of electrospun polymers reveals poly(3-hydroxybutyrate) fiber as a superior scaffold for cardiac repair. *Stem Cells Dev.* **2014**, *23*, 1479–1490. [CrossRef] [PubMed]

9. Serpooshan, V.; Zhao, M.; Metzler, S.A.; Wei, K.; Shah, P.B.; Wang, A.; Mahmoudi, M.; Malkovskiy, A.V.; Rajadas, J.; Butte, M.J.; et al. The effect of bioengineered acellular collagen patch on cardiac remodeling and ventricular function post myocardial infarction. *Biomaterials* **2013**, *34*, 9048–9055. [CrossRef] [PubMed]
10. Wang, Q.; Wang, H.; Li, Z.; Wang, Y.; Wu, X.; Tan, Y. Mesenchymal stem cell-loaded cardiac patch promotes epicardial activation and repair of the infarcted myocardium. *J. Cell. Mol. Med.* **2017**. [CrossRef] [PubMed]
11. Prabhakaran, M.P.; Kai, D.; Ghasemi-Mobarakeh, L.; Ramakrishna, S. Electrospun biocomposite nanofibrous patch for cardiac tissue engineering. *Biomed. Mater.* **2011**, *6*, 55001. [CrossRef] [PubMed]
12. Godier-Furnémont, A.F.G.; Martens, T.P.; Koeckert, M.S.; Wan, L.; Parks, J.; Arai, K.; Zhang, G.; Hudson, B.; Homma, S.; Vunjak-Novakovic, G. Composite scaffold provides a cell delivery platform for cardiovascular repair. *Proc. Natl. Acad. Sci. USA* **2011**, *108*, 7974–7979. [CrossRef] [PubMed]
13. Oberwallner, B.; Brodarac, A.; Choi, Y.-H.; Saric, T.; Anić, P.; Morawietz, L.; Stamm, C. Preparation of cardiac extracellular matrix scaffolds by decellularization of human myocardium. *J. Biomed. Mater. Res. Part A* **2014**, *102*, 3263–3272. [CrossRef]
14. Oberwallner, B.; Anic, B.A.; Šaric, W.; Kneef, K.; Choi, Y.-H.; Oberwallner, B.; Brodarac, A.; Anicá, P.; Šaric, T.; Wassilew, K.; et al. Human cardiac extracellular matrix supports myocardial lineage commitment of pluripotent stem cells. *Eur. J. Cardiothorac. Surg.* **2015**, *47*, 416–425. [CrossRef] [PubMed]
15. Kappler, B.; Anic, P.; Becker, M.; Bader, A.; Klose, K.; Klein, O.; Oberwallner, B.; Choi, Y.H.; Falk, V.; Stamm, C. The cytoprotective capacity of processed human cardiac extracellular matrix. *J. Mater. Sci. Mater. Med.* **2016**. [CrossRef] [PubMed]
16. Johnson, T.D.; Dequach, J.A.; Gaetani, R.; Ungerleider, J.; Elhag, D.; Nigam, V.; Behfar, A.; Christman, K.L. Human versus porcine tissue sourcing for an injectable myocardial matrix hydrogel. *Biomater. Sci.* **2014**, *2014*, 60283D. [CrossRef] [PubMed]
17. Johnson, T.D.; Hill, R.C.; Dzieciatkowska, M.; Nigam, V.; Behfar, A.; Christman, K.L.; Hansen, K.C. Quantification of decellularized human myocardial matrix: A comparison of six patients. *Proteom. Clin. Appl.* **2016**, *10*, 75–83. [CrossRef] [PubMed]
18. Chen, Q.-Z.; Bismarck, A.; Hansen, U.; Junaid, S.; Tran, M.Q.; Harding, S.E.; Ali, N.N.; Boccaccini, A.R. Characterisation of a soft elastomer poly(glycerol sebacate) designed to match the mechanical properties of myocardial tissue. *Biomaterials* **2008**, *29*, 47–57. [CrossRef] [PubMed]
19. Sicari, B.M.; Dziki, J.L.; Siu, B.F.; Medberry, C.J.; Dearth, C.L.; Badylak, S.F. The promotion of a constructive macrophage phenotype by solubilized extracellular matrix. *Biomaterials* **2014**, *35*, 8605–8612. [CrossRef] [PubMed]
20. Hansen, N.U.; Genovese, F.; Leeming, D.J.; Karsdal, M.A. The importance of extracellular matrix for cell function and in vivo likeness. *Exp. Mol. Pathol.* **2015**, *98*, 286–294. [CrossRef] [PubMed]
21. Ma, Y.; Halade, G.V.; Lindsey, M.L. Extracellular matrix and fibroblast communication following myocardial infarction. *J. Cardiovasc. Transl. Res.* **2012**, *5*, 848–857. [CrossRef] [PubMed]
22. Chen, W.C.W.; Wang, Z.; Missinato, M.A.; Park, D.W.; Long, D.W.; Liu, H.-J.; Zeng, X.; Yates, N.A.; Kim, K.; Wang, Y. Decellularized zebrafish cardiac extracellular matrix induces mammalian heart regeneration. *Sci. Adv.* **2016**, *2*, e1600844. [CrossRef] [PubMed]
23. Fong, A.H.; Romero-López, M.; Heylman, C.M.; Keating, M.; Tran, D.; Sobrino, A.; Tran, A.Q.; Pham, H.H.; Fimbres, C.; Gershon, P.D.; et al. Three-Dimensional Adult Cardiac Extracellular Matrix Promotes Maturation of Human Induced Pluripotent Stem Cell-Derived Cardiomyocytes. *Tissue Eng. Part A* **2016**, *22*, 1016–1025. [CrossRef] [PubMed]
24. Wang, Q.; Yang, H.; Bai, A.; Jiang, W.; Li, X.; Wang, X.; Mao, Y.; Lu, C.; Qian, R.; Guo, F.; et al. Functional engineered human cardiac patches prepared from nature's platform improve heart function after acute myocardial infarction. *Biomaterials* **2016**, *105*, 52–65. [CrossRef] [PubMed]
25. Sarig, U.; Sarig, H.; De-Berardinis, E.; Chaw, S.-Y.; Nguyen, E.B.V.; Ramanujam, V.S.; Thang, V.D.; Al-Haddawi, M.; Liao, S.; Seliktar, D.; et al. Natural myocardial ECM patch drives cardiac progenitor based restoration even after scarring. *Acta Biomater.* **2016**, *44*, 209–220. [CrossRef] [PubMed]
26. Slivka, P.F.; Dearth, C.L.; Keane, T.J.; Meng, F.W.; Medberry, C.J.; Riggio, R.T.; Reing, J.E.; Badylak, S.F.; Takeyama, H.; Feng, L.; et al. Fractionation of an ECM hydrogel into structural and soluble components reveals distinctive roles in regulating macrophage behavior. *Biomater. Sci.* **2014**, *2*, 1521–1534. [CrossRef] [PubMed]

27. Wolf, M.T.; Dearth, C.L.; Ranallo, C.A.; LoPresti, S.T.; Carey, L.E.; Daly, K.A.; Brown, B.N.; Badylak, S.F. Macrophage polarization in response to ECM coated polypropylene mesh. *Biomaterials* **2014**, *35*, 6838–6849. [CrossRef] [PubMed]
28. Dziki, J.L.; Wang, D.S.; Pineda, C.; Sicari, B.M.; Rausch, T.; Badylak, S.F. Solubilized extracellular matrix bioscaffolds derived from diverse source tissues differentially influence macrophage phenotype. *J. Biomed. Mater. Res. Part A* **2017**, *105*, 138–147. [CrossRef] [PubMed]
29. Williams, C.; Quinn, K.P.; Georgakoudi, I.; Black, L.D. Young developmental age cardiac extracellular matrix promotes the expansion of neonatal cardiomyocytes in vitro. *Acta Biomater.* **2014**, *10*, 194–204. [CrossRef] [PubMed]
30. Zhang, J.; Klos, M.; Wilson, G.F.; Herman, A.M.; Lian, X.; Raval, K.K.; Barron, M.R.; Hou, L.; Soerens, A.G.; Yu, J.; et al. Extracellular matrix promotes highly efficient cardiac differentiation of human pluripotent stem cells: The matrix sandwich method. *Circ. Res.* **2012**, *111*, 1125–1136. [CrossRef] [PubMed]
31. Faulk, D.M.; Londono, R.; Wolf, M.T.; Ranallo, C.A.; Carruthers, C.A.; Wildemann, J.D.; Dearth, C.L.; Badylak, S.F. ECM hydrogel coating mitigates the chronic inflammatory response to polypropylene mesh. *Biomaterials* **2014**, *35*, 8585–8595. [CrossRef] [PubMed]
32. Freytes, D.O.; Martin, J.; Velankar, S.S.; Lee, A.S.; Badylak, S.F. Preparation and rheological characterization of a gel form of the porcine urinary bladder matrix. *Biomaterials* **2008**, *29*, 1630–1637. [CrossRef] [PubMed]
33. Singelyn, J.M.; Sundaramurthy, P.; Johnson, T.D.; Schup-Magoffin, P.J.; Hu, D.P.; Faulk, D.M.; Wang, J.; Mayle, K.M.; Bartels, K.; Salvatore, M.; et al. Catheter-deliverable hydrogel derived from decellularized ventricular extracellular matrix increases endogenous cardiomyocytes and preserves cardiac function post-myocardial infarction. *J. Am. Coll. Cardiol.* **2012**, *59*, 751–763. [CrossRef] [PubMed]
34. Badylak, S.F.; Freytes, D.O.; Gilbert, T.W. Extracellular matrix as a biological scaffold material: Structure and function. *Acta Biomater.* **2015**, *5*, S17–S26. [CrossRef] [PubMed]
35. Tang, J.; Vandergriff, A.; Wang, Z.; Hensley, M.T.; Cores, J.; Allen, T.A.; Dinh, P.-U.; Zhang, J.; Caranasos, T.G.; Cheng, K. A Regenerative Cardiac Patch Formed by Spray Painting of Biomaterials onto the Heart. *Tissue Eng. Part C* **2017**, *23*. [CrossRef] [PubMed]
36. Du, J.; Zu, Y.; Li, J.; Du, S.; Xu, Y.; Zhang, L.; Jiang, L.; Wang, Z.; Chien, S.; Yang, C. Extracellular matrix stiffness dictates Wnt expression through integrin pathway. *Sci. Rep.* **2016**, *6*, 20395. [CrossRef] [PubMed]
37. Ribeiro, A.J.; Ang, Y.S.; Fu, J.D.; Rivas, R.N.; Mohamed, T.M.; Higgs, G.C.; Srivastava, D.; Pruitt, B.L. Contractility of single cardiomyocytes differentiated from pluripotent stem cells depends on physiological shape and substrate stiffness. *Proc. Natl. Acad. Sci. USA* **2015**, *112*, 12705–12710. [CrossRef] [PubMed]
38. Grotenhuis, N.; Toom, H.F.E.; Kops, N.; Bayon, Y.; Deerenberg, E.B.; Mulder, I.M.; van Osch, G.J.V.M.; Lange, J.F.; Bastiaansen-Jenniskens, Y.M. In vitro model to study the biomaterial-dependent reaction of macrophages in an inflammatory environment. *Br. J. Surg.* **2014**, *101*, 983–992. [CrossRef] [PubMed]
39. Ariganello, M.B.; Simionescu, D.T.; Labow, R.S.; Michael Lee, J. Macrophage differentiation and polarization on a decellularized pericardial biomaterial. *Biomaterials* **2011**, *32*, 439–449. [CrossRef] [PubMed]
40. Poss, K.D.; Wilson, L.G.; Keating, M.T. Heart regeneration in zebrafish. *Science* **2002**, *298*, 2188–2190. [CrossRef] [PubMed]
41. Kikuchi, K.; Holdway, J.E.; Werdich, A.A.; Anderson, R.M.; Fang, Y.; Egnaczyk, G.F.; Evans, T.; Macrae, C.A.; Stainier, D.Y.; Poss, K.D. Primary contribution to zebrafish heart regeneration by gata4(+) cardiomyocytes. *Nature* **2010**, *464*, 601–605. [CrossRef] [PubMed]
42. Gaetani, R.; Feyen, D.A.M.; Verhage, V.; Slaats, R.; Messina, E.; Christman, K.L.; Giacomello, A.; Doevendans, P.A.F.M.; Sluijter, J.P.G. Epicardial application of cardiac progenitor cells in a 3D-printed gelatin/hyaluronic acid patch preserves cardiac function after myocardial infarction. *Biomaterials* **2015**, *61*, 339–348. [CrossRef] [PubMed]
43. Chen, Q.Z.; Ishii, H.; Thouas, G.A.; Lyon, A.R.; Wright, J.S.; Blaker, J.J.; Chrzanowski, W.; Boccaccini, A.R.; Ali, N.N.; Knowles, J.C.; et al. An elastomeric patch derived from poly(glycerol sebacate) for delivery of embryonic stem cells to the heart. *Biomaterials* **2010**, *31*, 3885–3893. [CrossRef] [PubMed]
44. Moerkamp, A.T.; Lodder, K.; van Herwaarden, T.; Dronkers, E.; Dingenouts, C.K.; Tengstrom, F.C.; van Brakel, T.J.; Goumans, M.J.; Smits, A.M. Human fetal and adult epicardial-derived cells: A novel model to study their activation. *Stem Cell Res. Ther.* **2016**, *7*, 174. [CrossRef] [PubMed]

45. Becker, M.; Maring, J.A.; Oberwallner, B.; Kappler, B.; Klein, O.; Falk, V.; Stamm, C. Processing of Human Cardiac Tissue Toward Extracellular Matrix Self-assembling Hydrogel for In Vitro and In Vivo Applications. *J. Vis. Exp.* **2017**. [CrossRef] [PubMed]
46. Claycomb, W.C.; Lanson, N.A.; Stallworth, B.S.; Egeland, D.B.; Delcarpio, J.B.; Bahinski, A.; Izzo, N.J. HL-1 cells—A cardiac muscle cell line that contracts and retains phenotypic characteristics of the adult cardiomyocyte. *Proc. Natl. Acad. Sci. USA* **1998**, *95*, 2979–2984. [CrossRef] [PubMed]

LEBENSLAUF

Mein Lebenslauf wird aus datenschutzrechtlichen Gründen in der elektronischen Version meiner Arbeit nicht veröffentlicht.

KOMPLETTE PUBLIKATIONSLISTE

Forschungsartikel in Peer-Reviewed Journalen

Becker, M et al. Human cardiac ECM supplements a vital function for polymer-based epicardial patch designs – *in progress*

Becker, M., Schneider, M., Stamm, C., & Seifert, M. (2019). A polymorphonuclear leukocyte assay to assess implant immunocompatibility. *Tissue Engineering Part C: Methods*, *25*(8), 500-511.

Becker, M., Maring, J. A., Schneider, M., Herrera Martin, A. X., Seifert, M., Klein, O., ... & Stamm, C. (2018). Towards a Novel Patch Material for Cardiac Applications: Tissue-Specific Extracellular Matrix Introduces Essential Key Features to Decellularized Amniotic Membrane. *International journal of molecular sciences*, *19*(4), 1032.

Becker, M., Maring, J. A., Oberwallner, B., Kappler, B., Klein, O., Falk, V., & Stamm, C. (2017). Processing of Human Cardiac Tissue Toward Extracellular Matrix Self-assembling Hydrogel for In Vitro and In Vivo Applications. *Journal of visualized experiments: JoVE*, (130).

Kappler, B., Anic, P., **Becker, M**., Bader, A., Klose, K., Klein, O., ..., Stamm, C. (2016). The cytoprotective capacity of processed human cardiac extracellular matrix. *Journal of Materials Science: Materials in Medicine*, *27*(7), 1-13.

Roy, R., Haase, T., Ma, N., Bader, A., **Becker, M**., Seifert, M., ... & Stamm, C. (2016). Decellularized amniotic membrane attenuates postinfarct left ventricular remodeling. *Journal of Surgical Research*, *200*(2), 409-419.

Abstrakts für wissenschaftliche Konferenzen

DGTHG 2019

Becker, M., Maring, A. J., Klein, O., Falk, V., & Stamm, C. (2019). Controlled Epicardial Angiogenic Factor Stimulation for Improved Cardiac Regeneration upon Infarction via a Novel Biologic Patch. The Thoracic and Cardiovascular Surgeon, 67(S 01), DGTHG-KV151.

Becker, M., Somesh, D., Klose, K., Herrera, A. M., Klein, O., Jürchott, K., ... & Stamm, C. (2019). Human Cardiac ECM Hydrogel Coated Biological Scaffold upon Infarction Tailored for Epicardial Regeneration upon Infarction by Colonization of Transdifferentiated Cardiac Progenitors. The Thoracic and Cardiovascular Surgeon, 67(S 01), DGTHG-KV148.

BSRT Symposium 2018

Becker M, Schneider M, Klein O, Seifert M, Falk V, Stamm C; Polymorphonuclear cells (PMN) as a model for prediction of rejection

GSCN 2018

Matthias Becker, Dipthi Bachamanda Somesh, Kristin Klose, Aarón X. Herrera Martin, Olivia Reidell, Oliver Klein, Karsten Jürchott, Manfred Gossen, Volkmar Falk, Christof Stamm; Guided epicardial cell transfer of induced Cardiomyocyte Progenitors (iCMP) by human cardiac ECM hydrogel coated biological scaffold upon infarction

TERMIS 2017
Becker M, Schneider M, Maring JA, Seifert M, Ma N, Tung WT, Falk V, Stamm C; Human cardiac extracellular matrix coating improves the bioactivity of scaffolds designed to support myocardial regeneration processes. eCells & Materials (eCM) online journal

TermX-Meeting 2017
Becker M, Schneider M, Maring JA, Seifert M, Ma N, Tung WT, Falk V, Stamm C; Human cardiac extracellular matrix coating represents a successful strategy to increase cardiac specificity of epicardial biological and polymeric scaffolds

DGK 2017
Becker M, Schneider M, Tung WT, Falk V, Ma N, Seifert M, Stamm C; Human myocardial extracellular matrix coating improves biocompatibility of biologic and polymeric tissue engineering scaffolds. Clin Res Cardiol 106, Suppl 1, April 2017-P414. DOI: 10.1007/s00392-017-1105-2.

DGTHG 2017
Becker, M., Schneider, M., Maring, J., Seifert, M., Falk, V., & Stamm, C.; Processed Human Extracellular Matrix Coating of Human Amniotic Epicardial Patch Material Modulates Its Immunomodulatory Capacity Thorac cardiovasc Surg 2017; 65(S 01): S1-S110. DOI: 10.1055/s-0037-1598936

BSRT Symposium 2017
Becker M, Maring JA, Klein O, Falk V, Stamm C; Human cardiac extracellular matrix coated biological scaffolds provide a novel optimized epicardial application system using epicardial derived cells with r cardio-protective capacity

ESAO 2016
Becker M, Kappler B, Ma N, Falk V, Stamm C; Processing of human extracellular myocardial matrix preserves its cytoprotective effects. Int J Artif Organs 2016; 39(7): 321-357. DOI: 10.5301/ijao.5000507

BSRT Symposium 2016
Becker M, Schneider M, Maring JA, Seifert M, Stamm C; Human extracellular matrix enhances the biocompatibility of human amniotic membrane as a carrier material for epicardial regeneration purposes

DGTHG 2016
Becker M, Bader A, Roy R, Seifert M, Choi YH, Falk V, Ma N, Stamm C. Modulation of the Post-Infarct Immune Response by Epicardial Application of Decellularized Amniotic Membrane. Thorac cardiovasc Surg 2016; 64 - ePP29. DOI: 10.1055/s-0036-1571712

Becker M, Kappler B, Klose K, Choi YH, Falk V, Stamm C. Hydrogel Derived from Human Cardiac ECM Microparticles Exerts Superior Cytoprotective Effects. Thorac cardiovasc Surg 2016; 64 - ePP28. DOI: 10.1055/s-0036-1571711

DANKSAGUNG

Ich möchte mich an dieser Stelle ganz herzlich bei meinem Betreuer Prof. Christof Stamm bedanken, der mir die Möglichkeit gegeben hat in seiner Arbeitsgruppe zu arbeiten und mir zudem dieses spannende und interessante Thema gegeben hat.
Außerdem möchte ich mich bei Prof. Martina Seifert sowie meiner Mentorin Janita Aline Maring bedanken, die mich beide sowohl wissenschaftlich als auch menschlich sehr unterstützt und in kritischen Situation mit Rat und Tat begleitet haben.
Ein großer Dank gebührt ebenfalls Maria Schneider mit der ich nicht nur erfolgreich ein neues Projekt ins Leben rufen und Fördermittel einwerben konnte, sondern mit der ich sehr freundschaftlich und erfolgreich zusammenarbeiten und publizieren konnte.
Auch muss ich Sabine Bartosch dankend hervorheben. Als Koordinatorin der Graduiertenschule hatte sie immer ein offenes Ohr auch für Belange, die nichts mit Promotion und Wissenschaft zu tun hatten und war hierbei immer eine wichtige Unterstützung.
Allen Mitgliedern der Arbeitsgruppe Stamm möchte ich ebenfalls danken, die mir eine sehr angenehme Zusammenarbeit ermöglichten und mir in allen Situationen mit ihrer fachlichen Unterstützung zur Seite standen

Zuletzt aber möchte ich besonders und von ganzem Herzen meinen Eltern, meiner Familie und Freunden danken, die mich die gesamte Zeit der Promotion mit all ihren Möglichkeiten unterstützt haben und mir jederzeit mit Geduld und Verständnis zur Seite standen.